



Mas-Moruno, C., Su, B., & Dalby, M. J. (2019). Multifunctional Coatings and Nanotopographies: Toward Cell Instructive and Antibacterial Implants. *Advanced Healthcare Materials*, 8(1), [1801103].
<https://doi.org/10.1002/adhm.201801103>

Peer reviewed version

Link to published version (if available):
[10.1002/adhm.201801103](https://doi.org/10.1002/adhm.201801103)

[Link to publication record in Explore Bristol Research](#)
PDF-document

This is the author accepted manuscript (AAM). The final published version (version of record) is available online via Wiley at <https://doi.org/10.1002/adhm.201801103> . Please refer to any applicable terms of use of the publisher.

University of Bristol - Explore Bristol Research

General rights

This document is made available in accordance with publisher policies. Please cite only the published version using the reference above. Full terms of use are available:
<http://www.bristol.ac.uk/pure/about/ebr-terms>

Advanced Healthcare Materials

Multifunctional coatings and nanotopographies: towards cell instructive and antibacterial implants

--Manuscript Draft--

Manuscript Number:	adh.m.201801103R1
Full Title:	Multifunctional coatings and nanotopographies: towards cell instructive and antibacterial implants
Article Type:	Invited Review
Section/Category:	
Keywords:	implant coatings; osseointegration; infection; nanotopographies; multifunctional coatings
Corresponding Author:	Carles Mas-Moruno Universitat Politècnica de Catalunya Barcelona, Catalonia SPAIN
Additional Information:	
Question	Response
Please submit a plain text version of your cover letter here.	<p>Dear Dr. Bayindir-Buchhalter,</p> <p>In response to the conversation we had last year at the 2017 ESB, and the invitation to contribute with a Review to Advanced Healthcare Materials, I am very pleased to submit our review entitled "Multifunctional coatings and nanotopographies: towards cell instructive and antibacterial implants", co-authored by Dr. C. Mas-Moruno, Prof. B. Su and Prof. M. Dalby, for your consideration for publication in this journal.</p> <p>Our review focuses on the timely topic of simultaneously addressing the two major reasons of failure of dental and orthopedic implants: poor osteointegration and bacterial infection. Despite great advances in this field, many implant surfaces that support osteointegration have been found to also favor bacterial colonization. Conversely, efforts towards inhibiting bacteria may negatively affect host tissues and osteoblastic functions. However, the majority of current approaches, and works published, focus on either improving cell adhesion or preventing bacterial infection, but rarely explore a combined goal.</p> <p>The aim of this review is to provide an overview of strategies of surface modification to both improve implant biointegration and mitigate bacterial infections. Moreover, this review covers two emerging solutions, the use of multifunctional chemical coatings and nanotopographical features, which are seldom discussed in combination.</p> <p>We believe this review is unique in content and thus we expect will have a high impact in the scientific community, attracting a great deal of attention from researchers in the biomaterials and biomedical engineering sciences, and have a great number of citations. We will be very grateful if you consider our work for publication in Advanced Healthcare Materials.</p> <p>Best regards, Dr. C. Mas-Moruno</p>
Do you or any of your co-authors have a conflict of interest to declare?	No. The authors declare no conflict of interest.

Corresponding Author Secondary Information:	
Corresponding Author's Institution:	Universitat Politècnica de Catalunya
Corresponding Author's Secondary Institution:	
First Author:	Carles Mas-Moruno
First Author Secondary Information:	
Order of Authors:	Carles Mas-Moruno
	Bo Su
	Matthew Dalby
Order of Authors Secondary Information:	
Abstract:	In biomaterials science, it is nowadays well accepted that improving the biointegration of dental and orthopedic implants with surrounding tissues is a major goal. However, implant surfaces that support osteointegration may also favor colonization of bacterial cells. Infection of biomaterials and subsequent biofilm formation can have devastating effects and reduce patient quality of life, representing an emerging concern in healthcare. Conversely, efforts towards inhibiting bacterial colonization may impair biomaterial-tissue integration. Therefore, to improve the long-term success of medical implants, biomaterial surfaces should ideally discourage the attachment of bacteria without affecting eukaryotic cell functions. However, most current strategies seldom investigate a combined goal. This work reviews recent strategies of surface modification to simultaneously address implant biointegration while mitigating bacterial infections. To this end, two emerging solutions are considered, multifunctional chemical coatings and nanotopographical features.

DOI: 10.1002/ ((please add manuscript number))

Article type: Review

Multifunctional coatings and nanotopographies: towards cell instructive and antibacterial implants

Carlos Mas-Moruno, Bo Su and Matthew J. Dalby*

Dr. C. Mas-Moruno

Biomaterials, Biomechanics and Tissue Engineering Group, Department of Materials Science and Engineering & Center in Multiscale Science and Engineering, Universitat Politècnica de Catalunya (UPC), Barcelona, 08019, Spain

E-mail: carles.mas.moruno@upc.edu

Prof. Dr. B. Su

Bristol Dental School, University of Bristol, Bristol, BS1 2LY, United Kingdom.

Prof. Dr. M. J. Dalby

Centre for Cell Engineering, University of Glasgow, Glasgow, G12, Scotland, United Kingdom.

Keywords: implant coatings, osseointegration, infection, nanotopographies, multifunctional coatings

Abstract: In biomaterials science, it is nowadays well accepted that improving the biointegration of dental and orthopedic implants with surrounding tissues is a major goal. However, implant surfaces that support osteointegration may also favor colonization of bacterial cells. Infection of biomaterials and subsequent biofilm formation can have devastating effects and reduce patient quality of life, representing an emerging concern in healthcare. Conversely, efforts towards inhibiting bacterial colonization may impair biomaterial-tissue integration. Therefore, to improve the long-term success of medical implants, biomaterial surfaces should ideally discourage the attachment of bacteria without affecting eukaryotic cell functions. However, most current strategies seldom investigate a combined goal. This work reviews recent strategies of surface modification to simultaneously address implant biointegration while mitigating bacterial infections. To this end, two emerging solutions are considered, multifunctional chemical coatings and nanotopographical features.

1. Introduction

The replacement and healing of non-functional tissues has become a major challenge worldwide, due to the increase in life expectancy and the prevalence of age-related diseases. In the case of osteoarticular conditions, > 1 million total knee and hip replacement surgeries were performed in 2010 in the United States,^[1,2] and projections indicate that the number of primary and revision joint arthroplasties will grow significantly in coming years;^[3] similar statistics are also found in Europe.^[4,5] However, and despite the intrinsic capacity of bone to regenerate after injury, complete fracture healing and implant fixation are not always possible.^[6,7] Thus, joint replacements still fail at unacceptable rates, with some reports describing revision rates as high as 17.5% for total hip arthroplasty.^[8]

Successful implant fixation and full recovery of lost function depend on many factors, which include patient characteristics (e.g. age, alcohol consumption, smoking habits, metabolic conditions), factors associated with the implantation site (e.g. injury and infection at the site, poor vascularization) and those related to the surgical procedure and implant properties.^[9] Nonetheless, it is increasingly accepted that the two major causes of implant failure are aseptic loosening and infection.^[10] For example, a recent epidemiologic study indicates that mechanical loosening (20.3%) and infection (20.4%) were the most common etiology for revision of total knee arthroplasty in the United States between 2009 and 2013.^[11]

Incomplete osteointegration (i.e. not achieving a strong and durable connection between periimplant bone and the implant surface)^[12] represents a major contribution towards aseptic loosening. Although Brånemark's description of osteointegration originally referred to titanium (Ti) dental implants, it is nowadays widely used for orthopedic implants as well. Osteointegration relies on i) mechanical interdigitation, which ensures the primary fixation of the implant with bone after surgery, and ii) cellular interactions at the surface level, which are responsible of promoting osteoconduction, osteoinduction and healing during the first 3-4 months.^[13] Both processes are crucial to ensure an optimal clinical outcome, i.e. bone healing, allowing the recovery of lost function and patient's mobility.

Implant infection also represents a major concern.^[14,15] In fact, post-implantation, patients are more susceptible to infection. This increased vulnerability relates to the fact that the efficacy of the immune system is locally reduced by the presence of a foreign body (e.g. a metallic implant) and to the predilection of bacteria to adhere to solid substrates.^[16] Thus, it only takes a few adherent bacteria to attach to the implant surface, grow and multiply to form a biofilm.^[17,18] This process is usually initiated by planktonic bacteria, which act as primary colonizers, and is followed by a second phase, in which

1 secondary (or late) colonizers are irreversibly bound to the surface and create a biofilm. Once
2 established, biofilms are highly resistant to the immune system and conventional drugs, such as
3 antibiotics, and may also spread and infect other tissues. This further affects patient morbidity and
4 even results in death in severe cases.^[19,20,21,22] Moreover, the emergence of antibiotic resistance, e.g.
5 methicillin-resistant *Staphylococcus aureus* (MRSA), poses a serious threat.^[14,19,23] Although the
6 numbers vary greatly depending on the surgical procedure and the type of device, infection of
7 orthopedic implants may occur in up to 5% of cases.^[9] In the case of dental implants, infection rates
8 are higher, reaching values of peri-implantitis or dental implant infections as high as 14%.^[24]

9 It is therefore not surprising that extensive research is being performed to tackle these two problems,
10 and a large number of strategies for surface modification have been described to either improve implant
11 osteointegration^[9,13,25,26,27,28,29] or reduce bacterial infection.^[9,14,24,30,31,32,33,34] However, the necessity
12 of simultaneously addressing both these limitations has only been highlighted recently.^[10,35,36,37]

13 The development of multifunctional strategies that promote osteointegration while mitigating bacterial
14 colonization is clearly important because both effects are necessary to ensure an optimal, long-term
15 functionality of medical implants. However, we note that this notion is not new. Already in the late
16 1980s, the attachment of host cells and bacteria to the implant surface was defined as a competitive
17 “race for the surface”.^[38] In such a scenario, the winner takes it all. If host eukaryotic cells colonize
18 the implant and proliferate faster, the resulting adherent cell layer will discourage bacterial attachment
19 and reduce the risk of infection. In contrast, if bacteria are able to adhere and produce biofilms, the
20 osteointegration of the implant will be seriously compromised.

21 Further, classical approaches focusing only on improving one biological effect might paradoxically be
22 detrimental for the other. Implant surfaces that promote osteointegration (e.g. rough surfaces) may also
23 facilitate an increased bacterial attachment. Conversely, bactericidal agents used to inhibit bacterial
24 infection may be toxic or impair normal host cell functions.^[9,10]

25 The aim of this review is to provide an overview of the existing strategies of surface modification that
26 simultaneously combine cell adhesive/osteoinductive and antibacterial properties. Implants with such
27 multifunctional potential would accelerate implant osteointegration and healing but minimize the risk
28 of early/late infections – thus improving their clinical outcome and reducing the number of revision
29 surgeries. To this end, this review particularly focuses on two emerging solutions, the use of
30 multifunctional chemical coatings and nanotopographical features.

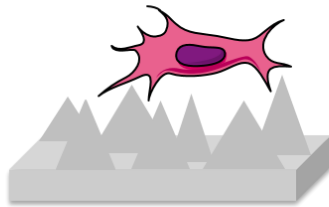
2. Classical strategies and limitations

2.1. Strategies to improve osteointegration

Improvement of the implant's bioactivity towards enhanced levels of osteointegration has been classically addressed by physical and chemical methods of surface modification (Figure 1A), and several reviews comprehensively covering these approaches are available.^[9,13,25,26,27,28,29]

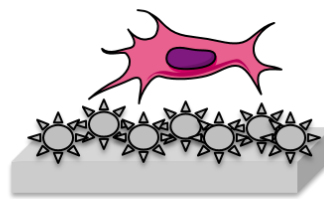
A Classical strategies to improve osteointegration

PHYSICAL MODIFICATIONS

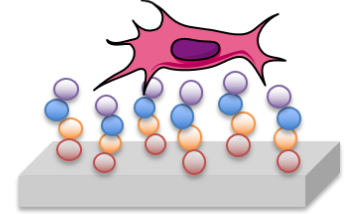


CHEMICAL MODIFICATIONS

Inorganic coatings

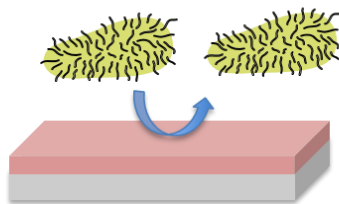


Organic coatings



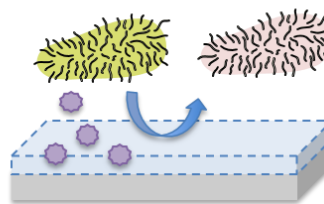
B Classical strategies to inhibit bacterial infection

PASSIVE COATINGS



ACTIVE COATINGS

Drug-releasing



Immobilized

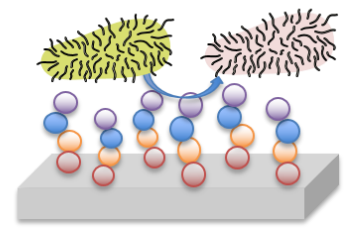


Figure 1: Schematic summary of classical strategies of surface functionalization. A) Improvement of osteointegration can be achieved by physical methods, which commonly focus on modifying the surface topography (e.g. surface roughness), or chemical methods, which are based on inorganic (e.g. calcium phosphate) or organic (e.g. peptide and protein) coatings. B) The strategies to inhibit bacterial infection can be divided into passive (e.g. anti-adhesive) or active (e.g. drug eluting or immobilized) coatings.

Physical methods have largely focused on increasing the average roughness (Ra) of the implant surface, following experimental evidence *in vivo* that substrates with higher Ra were capable of achieving higher rates of osteointegration.^[13,39] This observation may be due to higher micromechanical retention of bone on rougher substrates compared to smooth ones, and the positive influence of surface

1 roughness on protein adsorption and osteoblastic function.^[40,41,42] Increasing surface roughness at the
2 submillimeter – micrometer level can be easily achieved by several inexpensive methods, such as grit
3 blasting or acid etching, and many dental implants nowadays display Ra values within 1 to 5 μm . The
4 main limitation of non-specifically increasing the surface roughness of an implant above a certain
5 threshold (some authors have defined this value as $Ra > 0.2 \mu\text{m}$)^[43,44] is that such rougher surface will
6 likely support higher levels of bacterial attachment as well (Table 1). Alternatively, well-defined
7 surface modifications at the nanotopographic level have emerged – and are now established – as a
8 feasible way to control stem cell response and osteogenic differentiation. Topographical features at the
9 nanoscale are not expected to promote bacterial attachment (i.e. they are below $0.2 \mu\text{m}$) and can be
10 tuned to even prevent infection. This subject will be covered with detail in Sections 4 and 5 of this
11 review.
12
13
14
15
16
17
18
19

20 Chemical coatings generally try to mimic the extracellular matrix (ECM) of bone.^[27] As such,
21 inorganic coatings are often based on calcium phosphate (CaP) / hydroxyapatite (HAp), the mineral
22 component of bone. Organic coatings, on the other hand, include cell adhesive proteins or peptides
23 derived from the ECM. The deposition of CaP minerals to bioactivate implant surfaces has represented
24 a main focus of research for more than 30 years now.^[45,46] This was originally achieved by plasma
25 spray and electrodeposition methods,^[47,48] but concerns on the (poor) mechanical stability of thick CaP
26 coatings were later reported.^[49,50] To overcome this, biomimetic strategies were described during the
27 90s. In general, these strategies allowed the formation of thinner CaP layers, exhibiting high bioactivity
28 and better mechanical properties.^[51,52,53,54,55,56,57] A representative and successful example is the
29 method developed by Kokubo,^[51,58] which combines a basic etching and a thermal treatment of Ti to
30 produce an amorphous sodium titanate layer. Immersion of treated surfaces into physiological buffers
31 (i.e. simulated body fluid, SBF) drives the nucleation of bone-like apatite, thus conferring bioactivity
32 to the material. Interestingly, this method has shown good versatility and can be applied to other
33 medically-relevant materials, including niobium, tantalum and zirconium.^[59,60,61]
34
35
36
37
38
39
40
41
42
43
44
45

46 These coatings are highly osteoconductive and have shown osteointegrative potential *in vivo*.^[9,13]
47 According to some authors, CaP materials are osteoinductive as well, which may be attributed to their
48 capacity to adsorb proteins such as growth factors (GFs). In this regard, both their chemistry and
49 specific surface area can be tuned to efficiently immobilize bone morphogenetic proteins (BMPs) –
50 yet it is plausible that these characteristics (i.e. high specific surface area) may concomitantly favor
51 bacterial adhesion (Table 1).^[62] A potential solution to that is to use CaP coatings as drug delivery
52 systems (e.g. loaded with antibacterial agents),^[63] so the bioactivity of CaP can be combined with
53 antibacterial properties (this strategy will be discussed in Section 3.2).
54
55
56
57
58
59
60
61

1 Organic coatings include a diverse range of molecules, from polymers to proteins, peptides or small
2 organic molecules.^[13,64] In general, this strategy has focused on proteins from bone ECM, with
3 fibronectin, vitronectin and collagens being representative examples.^[27,28,65] The majority of ECM
4 proteins support cell attachment via cell adhesive motifs such as the RGD sequence,^[66,67] which
5 recognizes and binds to integrin receptors expressed by eukaryotic cells.^[68] Integrin (and non-integrin)
6 binding ligands have thus been frequently used not only to improve cell adhesion but also to stimulate
7 cell proliferation and differentiation.^[69,70] As the use of native ECM proteins and synthetic peptides
8 entails limitations of stability, biological potency and specificity (these issues still remain
9 controversial),^[71,72,73] advances in this field have focused on recombinant protein fragments,^[74,75,76,77]
10 multifunctional peptides^[78,79,80] and non-peptidic ligands.^[69,81]

11
12
13
14
15
16
17
18
19 Inducing integrin signaling cascades has become a common strategy to improve bone healing.
20 However, to optimally mimic the cellular microenvironment on the biomaterial surface, signaling
21 through other mechanisms is required. For instance, several GFs such as BMPs^[82] are known to
22 cooperate with integrin ligands to regulate bone regeneration. In this regard, a growing body of
23 evidence indicates that GF signaling can be regulated and enhanced by dynamic crosstalk with integrin
24 receptors.^[83,84,85] In particular, recent examples have shown that the combination of ECM proteins with
25 BMPs has a synergistic effect to induce stronger osteogenic signals and bone formation *in vivo* with
26 reduced doses of GF.^[86,87,88,89] These approaches are of relevance and constitute a hot topic of research,
27 as they take advantage of the osteoinductive potential of BMPs while overcoming the complications
28 and concerns associated to their use.^[90,91] Further information is available in the recent
29 literature.^[35,84,85]

30
31
32
33
34
35
36
37
38
39 Functionalization of medical implants with molecules from the ECM appears to provide a strategy that
40 should not promote bacterial colonization. However, organic coatings are not exempt from risks either.
41 For example, the production of proteins (or fragments) by recombinant methods is commonly done
42 using bacterial systems. Such methods inherently entail the risk of introducing remnants of bacteria
43 (e.g. endotoxins) on the biomaterial surface during the coating procedure. In addition, bacteria share
44 similar adhesion mechanisms with eukaryotic cells to attach to surfaces, and may bind to ECM proteins
45 such as fibronectin^[92,93] or collagens^[94].

46
47
48
49
50
51
52
53 Finally, it should be mentioned that the aforementioned strategies (e.g. surface roughness and bioactive
54 coatings) can be combined to achieve synergistic effects and improved biological responses. For
55 example, grit blasting of titanium surfaces,^[95] followed by alkaline etching and thermal treatments (a
56 method named *2Step*) showed accelerated *in vitro* formation of bioactive apatite on the bottom of the
57 topographical valleys in comparison to smooth surfaces.^[96] This treatment showed improved
58
59
60
61
62
63
64
65

1 differentiation of human osteoblastic cells *in vitro*^[97] and enhanced bone formation *in vivo*.^[13,98]
2 Another study evaluated the combination of different levels of surface roughness with a cyclic RGD
3 peptide. Interestingly, the highest levels of cell adhesion were obtained on the rougher surfaces
4 functionalized with the peptide, compared to peptide-coated smooth surfaces or non-functionalized
5 controls (smooth and rough).^[99]
6
7

8 **2.2. Strategies to inhibit bacterial infection**

9
10 The number of strategies investigated to fight bacterial infection is also growing, and this field
11 represents a very active area of research in the biomaterials community.^[9,14,24,30,31,32,33,34] Although a
12 myriad of methods have been described, a common classification is to divide antibacterial treatments
13 as passive or active, depending on their ability to discourage bacterial cell attachment or actually kill
14 contaminating bacteria, respectively. Active coatings may rely on the release of antibacterial agents
15 (release-based) or surface strategies (non-release-based) (Figure 1B). Regardless of classification, the
16 goal is always the same: inhibit bacterial adhesion on the surface and prevent the formation of highly
17 resistant biofilms.
18

19 Passive coatings are typically based on anti-adhesive polymers that prevent protein and cellular (e.g.
20 bacteria) attachment. Alternatively, such anti-fouling effect can also be achieved using
21 nanotopographies (see Section 5.1). Among all polymers, polyethylene glycol (PEG) is probably the
22 most widely used to confer anti-fouling properties to a material surface.^[30,100] Its repelling properties
23 are related to its flexible and hydrophilic chains. These chains form a wide exclusion volume that
24 blocks protein adsorption and cell attachment. Other examples of low fouling polymers include
25 poly(methacrylic acid) (PMAA), dextran or hyaluronic acid.^[36] Such coatings can easily be applied to
26 a broad range of materials and have the advantage of being simple, effective and not requiring the use
27 of drugs. However, the main strength of anti-adhesive coatings represents a concomitant weakness, as
28 very efficient bacteria repelling coatings will inhibit eukaryotic cell attachment as well. For this reason,
29 anti-fouling polymers often require the incorporation of cell adhesive sequences to preserve cell
30 adhesion and the biomaterial's functionality. Such strategy represents a clear example of
31 multifunctional coating and is described later in Section 3.1.
32
33

34 In contrast to passive coatings, active coatings exert their antibacterial action by directly killing
35 bacteria. This may be achieved by a very diverse range of molecules, including bactericidal polymers
36 (e.g. chitosan, cationic polymers), quaternary ammonium salts, ions (e.g. silver, zinc), antibiotics,
37 bactericidal agents (e.g. chlorhexidine) and antimicrobial peptides (AMPs).^[9,14,24,31,32,33,34] These
38 strategies are largely reliant upon two physicochemical approaches: i) the incorporation of antibacterial
39
40
41
42
43
44
45
46
47
48
49
50

agents (e.g. antibiotics or silver ions) on the biomaterial via physical adsorption or entrapment in polymeric matrices (drug-releasing mechanism), and ii) the covalent functionalization of the materials with bactericidal molecules (e.g. AMPs). Although drug-releasing approaches are commonly applied and have proven their efficacy in many reports, the second approach (i.e. immobilization of the antibacterial molecule) warrants further research because the release of antibacterial agents entails several risks in terms of (off target) toxicity, rapid dwindling concentration due to release and loss of activity over time; these latter effects necessitate use of very high doses increasing toxicity and increasing probability of bacterial resistance.

In particular, the emergence of antimicrobial resistance mechanisms in bacteria severely compromises the use of antibiotics and other antibacterial drugs.^[101,102] For instance, the highly virulent multi-drug resistant strains of *Staphylococcus aureus* (e.g. MRSA) establish dangerous infections that in many instances are very difficult or impossible to treat with existing medicines.^[103] These bacteria, also known as “superbugs”, are considered one of the most frequent causes of healthcare-associated infections worldwide and are responsible for a high mortality rate. As mentioned before, on biomaterial-associated infections, the picture is further complicated by the growth of biofilms, exacerbating the antibiotic resistance scenario. Furthermore, it has also been described that the release of antibacterial agents such as silver or antibiotics may negatively affect osteoblastic functions as well (Table 1).^[104,105]

Table 1. Summary of classical strategies of surface functionalization of biomaterials, main effect targeted and potential non-wanted effects.

Strategy	Main effect targeted	Limitation
Increasing surface roughness (e.g. Ra in the μm range)	Improvement of osteointegration by higher mechanical retention	Rough surfaces (e.g. $> 0.2 \mu\text{m}$) may also increase bacterial attachment
Inorganic coatings based on CaP / bone-like apatite	Providing osteoconductive / osteoinductive potential to improve osteointegration	Higher specific surface area of CaP may also increase bacterial attachment
Organic coatings based on proteins / peptides from the ECM	Providing osteoconductive / osteoinductive potential to improve osteointegration	Bacteria share cell adhesion mechanisms with eukaryotic cells (using ECM molecules)
Anti-adhesive coatings	Inhibiting / repelling bacterial attachment	Eukaryotic cell attachment is also compromised (inhibited)
Bactericidal coatings (release-based and non-release-based)	Killing bacteria / inhibiting bacterial attachment	Eukaryotic cell attachment, functions and viability may be also compromised

3. Multifunctional chemical coatings

The functionality of biomaterials can be significantly improved by either enhancing their interaction with eukaryotic cells (e.g. osteoblasts – improved osteointegration) or inhibiting bacterial infection. However, specifically improving host cell adhesion while inhibiting bacterial attachment is a challenging task. As a matter of fact, most approaches intended to confer osteoinductive properties to biomaterials have not considered the risk of bacterial colonization. Or worse, treatments or surface modifications that facilitate cell adhesion and proliferation, may also favor bacterial attachment and biofilm formation. Conversely, research efforts devoted to inhibit bacterial colonization are often related to anti-adhesive polymers or cytotoxic agents that may compromise osteoblast-like cell functions.

In this section, we will focus on coatings composed of distinct chemical entities (e.g. materials, biomolecules or drugs), which are combined in a way that a dual function (i.e. osteointegrative and antibacterial) is achieved. These strategies are normally not intended to modify the properties of the bulk material, only its surface, and hence are categorized as strategies of surface functionalization. Although the number of examples in the literature is rapidly increasing and a myriad of combinations are possible, we will center this section according to three differentiated approaches: i) antibacterial coatings functionalized with cell instructive molecules; ii) osteoconductive/osteoinductive coatings loaded with antibacterial agents; and iii) immobilized multifunctional peptides (Figure 2 and Table 2).

3.1 Coatings based on antibacterial polymers

3.1.1 Functionalized anti-adhesive polymers

The first approach to achieve cell instructive and antibacterial effects focuses on the use of anti-fouling polymers functionalized with cell adhesive peptides (Figure 2A). It is plausible that this strategy was originally not conceived as a multifunctional coating, but that it responded to the inherent limitations of anti-fouling polymers like PEG. As previously outlined, PEG is very efficient in preventing bacterial attachment, but it also blocks the adhesion of wanted host cells – as a matter of fact, PEG is frequently used to reduce non-specific cell binding in cellular and biophysical studies. Thus, the incorporation of a cell adhesive sequence such as RGD is required to maintain cell-binding properties.

To the best of our knowledge, the first report following this strategy was published by Harris and coworkers in 2004 (Table 2).^[106] In this work, PEG was electrostatically adsorbed on Ti surfaces using poly-L-lysine (PLL), and the PEG-PLL co-polymer was further functionalized with an RGD peptide using vinyl sulfone-thiol chemistry. The PEG coating significantly reduced the attachment of *Staphylococcus aureus*, and, of note, the presence of the RGD peptide did not affect the antibacterial

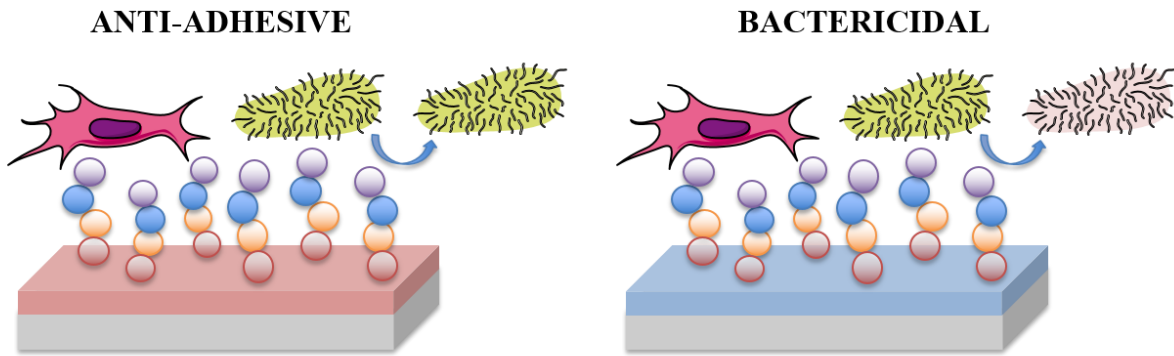
1 activity. In a subsequent study, the same group showed a reduced attachment of other medically
2 relevant bacterial strains (e.g. *Staphylococcus epidermidis*, *Streptococcus mutans* and *Pseudomonas*
3 *aeruginosa*).^[107] However, the authors did not check the response of eukaryotic cells to the RGD
4 peptide on these studies. Both effects were actually reported in other investigations, which reflected
5 the multifunctional potential of this strategy: the passive PEG layer inhibited bacterial attachment,
6 while the RGD peptide simultaneously supported (or improved) osteoblast (OB)^[108] or fibroblast
7 (FB)^[109] adhesion. In addition to electrostatic adsorption, a number of other methods have been
8 proposed to coat Ti surfaces with PEG, such as electrodeposition, silanization and plasma
9 polymerization.^[109]

10 This technique is facile and versatile, as it can be expanded using different anti-fouling polymers and
11 bioactive sequences. For instance, PMAA, dextran or hyaluronic acid have been combined with cell
12 adhesive sequences (e.g. RGD, silk sericin) or GFs (e.g. BMP-2, vascular endothelial growth factor,
13 VEGF) demonstrating excellent dual potential (see Table 2 for details).^[110, 111,112]

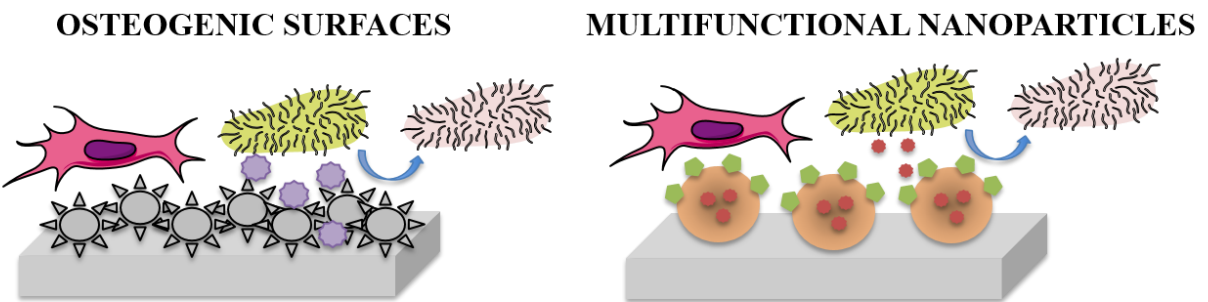
14 Recent studies have further combined the anti-adhesive properties of PEG and other polymers with
15 bactericidal agents (e.g. quaternary ammonium compounds, ions, AMPs or bactericidal polymers) to
16 simultaneously exploit passive and active antibacterial mechanisms.^[113,114,115,116,117,118,119] Such dual
17 antibacterial function aims at both preventing bacterial attachment and killing bacteria able to adhere.
18 This approach is also interesting because it inhibits the accumulation of bacterial debris and proteins,
19 which may provide anchoring points for the formation of biofilms. These works, however, do not
20 address eukaryotic cell adhesion – crucial to ensure implant integration with tissues – and will not be
21 covered in this review.

22 The major limitation of using polymers to coat substrates is the risk of polymer degradation over time.
23 Degradation may compromise the long-term stability and prolonged effect of the coatings. Moreover,
24 their fabrication and obtaining of defined and homogenous structures may be challenging.

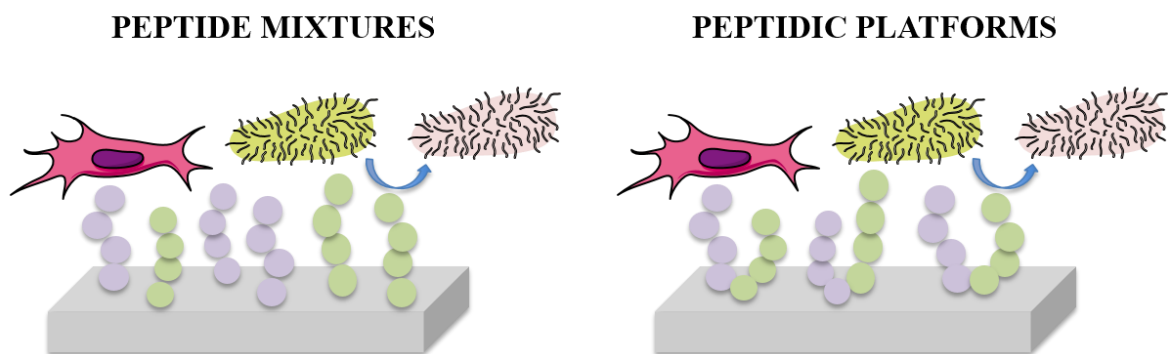
1 **A Antibacterial polymers**



18 **B Osteoconductive/osteoinductive (+ antibacterial agents)**



34 **C Immobilized peptides**



52 **Figure 2:** Schematic summary of multifunctional strategies to achieve both cell instructive and antibacterial
53 properties. A) Antibacterial polymers can be used to either repel (anti-adhesive, e.g. PEG) or kill (bactericidal,
54 e.g. chitosan) bacteria; in both cases the presence of a cell adhesive sequence is required; B) the opposite
55 approach is to use osteogenic surfaces (Ti dioxide nanotubes, TNTs, CaP coatings) or RGD-decorated
56 nanoparticles that incorporate and release antibacterial agents (e.g. antibiotics, silver, AMPs); C) A third strategy
57 is to covalently immobilize cell adhesive sequences and AMPs on the biomaterial surfaces. To this end, peptide
58 mixtures or peptidic branched platforms can be used.
59

3.1.2 Functionalized bactericidal polymers

1
2 An alternative strategy to anti-adhesive coatings like PEG is to use polymeric coatings that are directly
3 bactericidal. One canonical example is chitosan, which is well known for its antibacterial
4 properties.^[120] Although this polymer has been also attributed with good biocompatibility and cell
5 adhesive activity, several reports have combined chitosan with cell adhesive peptides to achieve a dual
6 effect; examples are provided in Table 2. For instance, Neoh and colleagues adsorbed polyelectrolyte
7 multilayers of chitosan and hyaluronic acid on Ti, and anchored an RGD peptide to the external
8 chitosan layer via carbodiimide chemistry. The resulting surfaces inhibited *Staphylococcus aureus*
9 adhesion while improving osteoblastic responses (adhesion, proliferation and alkaline phosphatase,
10 ALP, activity).^[121] In a parallel study, the same authors reported the covalent immobilization of RGD-
11 coated chitosan with very similar biological results.^[122] In this case, Ti was sequentially modified with
12 dopamine (which binds to Ti via the catechol moiety) and glutaraldehyde, rendering a free aldehyde
13 group on the surface that was used to covalently bind chitosan by reductive amination. The RGD
14 sequence was finally grafted using carbodiimide chemistry. Another viable solution is to immobilize
15 GFs or enzymes onto chitosan layers to improve cell adhesion and also osteogenic differentiation. This
16 has been achieved using combining chitosan or carboxymethyl chitosan and with BMP-2^[123,124],
17 VEGF^[112] or ALP^[125] (see Table 2 for details). The biological potential of chitosan can be further
18 increased with other antibacterial agents. In a recent study, the combination of chitosan with gallium
19 effectively decreased *Escherichia coli* and *Pseudomonas aeruginosa* viability. Interestingly, gallium
20 also showed a beneficial osteogenic effect.^[126]

21
22 In addition to chitosan, a number of other antibacterial cationic polymers have been described, such as
23 ϵ -poly-L-lysine (ϵ -PLL), quaternary ammonium polymers, polyethylenimine and polyguanidines.^[127]
24 Among them, ϵ -PLL has shown a broad spectrum of antimicrobial activity against Gram-negative and
25 Gram-positive bacteria but low toxicity for eukaryotic cells.^[127,128] Taking advantage of this, ϵ -PLL-
26 based hydrogels with wound healing and anti-infective properties have been developed.^[129,130] As
27 positively charged polymers easily adsorb electrostatically on oxidized metallic surfaces, it is expected
28 that these polymers may also be used as multifunctional coatings on orthopedic implants.

3.2 Osteoconductive/osteoinductive surfaces loaded with antibacterial agents

A conceptually similar but inverse approach is to use surfaces that have osteoconductive or osteoinductive potential. Coatings such as Ti dioxide nanotubes (TNTs) or CaP can be doped with antibacterial agents, such as antibiotics or cations.

TNTs represent a very attractive strategy in the biomedical field as they have excellent corrosion resistance and biocompatibility. In particular, they have been described to improve osteoblastic functions and, in some cases, have antibacterial potential (although these effects are largely reliant on the TNTs geometry and physicochemical properties).^[131] On the basis of these interesting features, TNTs have been fabricated by different methods (e.g. template-assisted, anodization or hydrothermally) and loaded with silver (either as ion^[132] or nanoparticles^[133,134]), zinc^[135,136], copper^[137] or antibiotics.^[138,139] Overall, this approach has shown good biocompatibility with OB-like cells, improved osteogenic responses and reduced adhesion and viability of several bacterial strains (Table 2). For this type of system, a crucial parameter to control is the concentration of the molecule released, as it has been observed that the release of high concentrations of silver may be cytotoxic for several eukaryotic cell types (e.g. epithelial cells, FBs and OBs),^[133,140] and that high doses of ZnO and silver nanoparticles may decrease the antibacterial activity or even promote bacterial attachment.^[141] Moreover, recent evidence has shown that certain bacterial isolates may develop resistance to silver.^[142] Alternatively, TNTs can be engineered in a way that support the adhesion of osteogenic cells but reduce bacterial attachment without the addition of ions (see Section 6 for details).^[143,144]

A more classical approach would be to employ CaP coatings, which are inherently osteoconductive, and load them with antibacterial agents. Here, silver is frequently used too.^[145,146,147,148,149] For example, HAp coatings doped with Ag₂O and SrO were plasma-sprayed onto Ti to incorporate bactericidal potential to the inorganic substrate. Interestingly, silver was highly effective against *Pseudomonas aeruginosa* but the release of this ion was detrimental for the activity of OBs. Co-doping the coating with SrO seemed to compensate this negative effect and rescued normal osteoblastic functions (Table 2).^[150] Thus, the antibacterial potential of silver can be combined with the bioactivity of strontium within CaP-based coatings to improve Ti implants response; recent reports have further exploited such interesting multifunctional approach.^[151,152] The limitations described for silver in the previous examples can be circumvented using other antibacterial agents. For example, AMPs (HHC36: KRWWKWWRR; Tet213: KRWWKWWRRRC) have been incorporated into CaP coatings.^[153,154] While Tet213 showed toxicity for OB-like cells even at low concentrations, HHC36 displayed little toxicity. HHC36-CaP-coated Ti surfaces showed antibacterial potential against *Staphylococcus aureus*

1 and *Pseudomonas aeruginosa* and improved levels of osteoconductivity in an *in vivo* model of
2 trabecular bone growth using cylindrical implants in rabbits.^[154] This study suggests that AMPs may
3 be a good alternative to silver but also shows that the selection of the peptide is important (i.e. balancing
4 good antibacterial activity with low toxicity for eukaryotic cells). Antibiotics have also been frequently
5 combined with CaP coatings showing effective osteoconductivity and antibacterial properties.^[63]
6 Diverse examples of this strategy can be found in the literature and include the use of gentamicin,^[155]
7 vancomycin^[156,157] and its derivatives,^[158] among others.

8
9
10
11
12
13
14 Regardless of the antibacterial agent used, a common limitation of this approach is the burst release of
15 the bactericide. Such rapid release may be deleterious for several reasons, i) it reduces the long-term
16 effectiveness of the coatings; ii) a high concentration of drug may be toxic for host cells; and iii) it
17 may promote bacterial resistance. A potential solution to this problem is to introduce polymeric
18 coatings that cap and protect the coating, and that deliver the drug as they degrade, thus slowing down
19 release kinetics. For example, this has been achieved with polylactic-*co*-glycolic acid (PLGA), which
20 was used to control the delivery of the antibiotic clindamycin from different CaP coatings.^[159] A
21 similar polymeric coating was used to fine-tune the release of drugs from TNTs.^[138] In this case, TNTs
22 were loaded with gentamicin and subsequently covered by PLGA and chitosan coatings (Figure 3).^[138]
23 Interestingly, the polymeric coatings not only improved the drug-release kinetics (i.e. decreased burst
24 release) but also enhanced OB-like cell adhesion and reduced bacterial viability, representing an
25 elegant example of tri-functional coating (e.g. TNT + antibiotic + chitosan). Similarly, the release of
26 an AMP from a TNT-CaP coating was tuned using a phospholipid (1-palmitoyl-2-oleoyl-*sn*-glycero-
27 3-phosphocholine, POPC) capping layer.^[160] Regulating the delivery of drugs from biomaterials with
28 polymeric coatings is not easy and depends on many factors (e.g. the degradability of the polymer and
29 stability, its chemistry, the number of layers deposited...) but opens new avenues to finely control the
30 antibacterial action, ensuring prolonged effects and reducing unspecific toxicity. As new methods
31 become available, a higher control might be possible. One of such methods is plasma polymerization,
32 which has recently shown to be very effective in tuning the release of antibiotics from different
33 biomaterials.^[161,162]

1
2
3
4
5
6
7
8
9
10
11
12
13
14
15
16
17
18
19
20
21
22
23
24
25
26
27
28
29
30
31
32
33
34
35
36
37
38
39
40
41
42
43
44
45
46
47
48
49
50
51
52
53
54
55
56
57
58
59
60
61
62
63
64
65

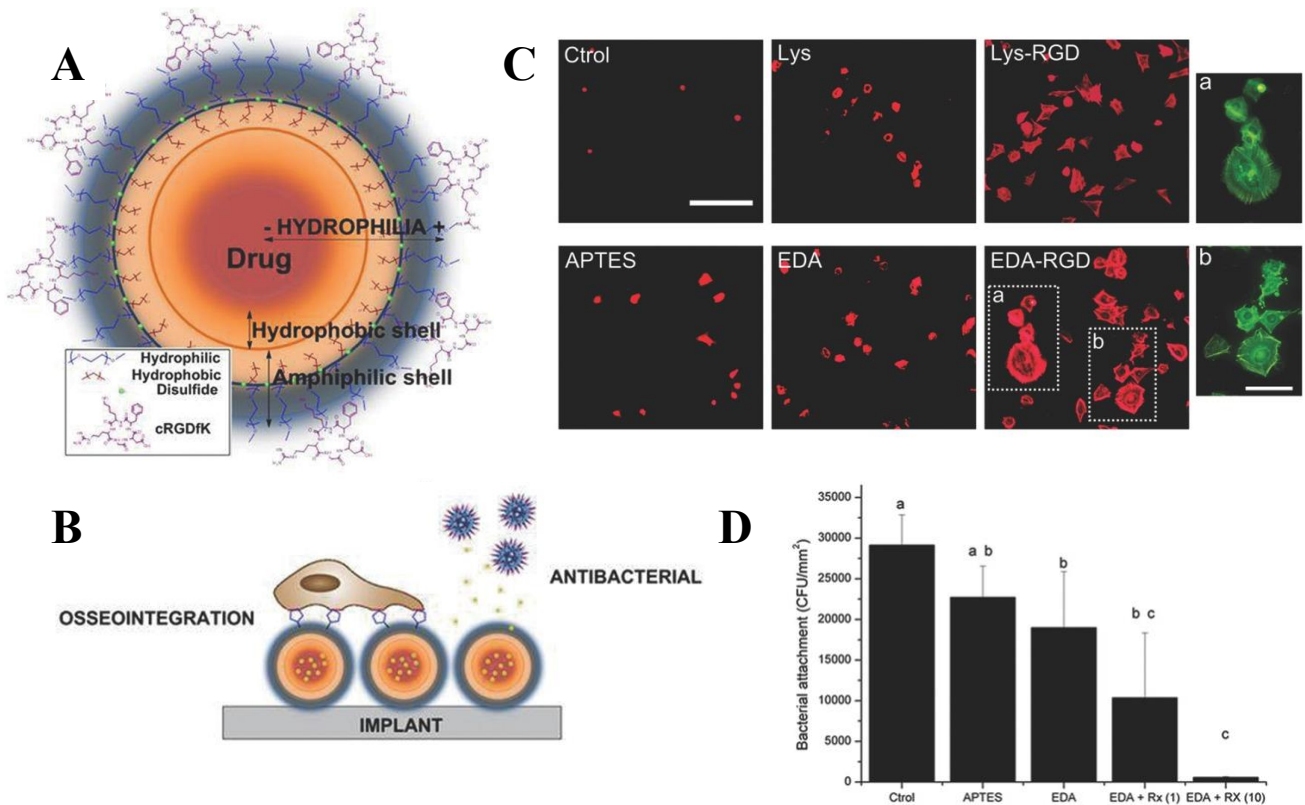


Figure 4: A) Schematic representation of the multifunctional nanoparticles (NPs). The combination of hydrophilic and hydrophobic moieties confers an amphipathic structure to the NP. The drug roxithromycin is encapsulated in the hydrophobic oily core of the NP and the surface is decorated with the cyclic RGD peptide c(RGDfK). B) Multifunctional activity of the NPs. C) Immunostaining of OB-like cells on Ti; the samples functionalized with RGD-decorated NPs promoted higher cell adhesion and focal adhesions than controls; D) Antibacterial effect of the coatings. Roxithromycin significantly inhibits *Streptococcus sanguinis* attachment in a concentration-dependent manner. Ctrl: Ti non-functionalized; APTES: Ti aminosilanized; Lys/EDA (ethylenediamine): Ti functionalized with NPs (different crosslinker used) without RGD; Lys/EDA-RGD: Ti functionalized with RGD-NPs. **Reproduced (adapted) from [164].**

In this regard, we recently described the use of RGD-decorated polyurethane-polyurea nanoparticles loaded with the antibiotic roxithromycin as multifunctional systems to functionalize Ti (Figure 4).^[164] The multifunctional nanoparticles enhanced OB-like adhesion (cell numbers, spreading and focal adhesion formation) and proliferation compared to plain Ti and Ti functionalized with nanoparticles without the RGD motif. Simultaneously, the nanoparticles strongly suppressed the adhesion of *Streptococcus sanguinis* on the surfaces in a concentration (i.e. of roxithromycin)-dependent manner. The nanoparticles released 60-70% of the drug within the first 4-6 h, which would address the elevated risk of infection post-implantation,^[165,166] but the remaining drug was released very slowly, allowing a sustained antibacterial effect at longer time periods. Interestingly, the remaining ca. 30% of drug was still efficient at inhibiting bacterial colonization at longer time points. Such design would thus tackle both acute infections post-surgery and chronic defense mechanisms; however, the application of this strategy on biomaterials remains to be fully explored.

1 Bovine serum albumin (BSA)-based nanoparticles (BNPs) are also gaining increasing attention as
2 multifunctional systems with the capacity to control the release of diverse drugs. In a recent report, Lu
3 and coworkers described nanostructured architectures on Ti surfaces by alternating layers of BNPs
4 loaded with either BMP-2 or vancomycin.^[167] The coatings were produced following a layer-by-layer
5 approach, as BNPs were coated with chitosan or oxidized alginate to render positively or negatively
6 charged BNPs, respectively. These coatings allowed a long-term sustained release of the drugs and
7 showed a remarkable multifunctional potential: while the nanostructured texture and BMP-2 promoted
8 BMSC adhesion, proliferation and osteogenic differentiation (i.e. increased ALP activity), vancomycin
9 inhibited the growth of *Staphylococcus epidermidis* up to 7 days of incubation (Table 2).^[167] These
10 systems are versatile and can be used to encapsulate other substances. For example, in another study
11 of the same group, BNPs-coated with chitosan and loaded with dexamethasone were combined with
12 vancomycin-conjugated alginate to produce films with osteoinductive and antibacterial properties.^[168]
13
14
15
16
17
18
19
20
21
22
23
24

25 3.3 Immobilization of peptides

26
27 The last multifunctional strategy focuses on the covalent immobilization of peptides. This approach,
28 together with the use of nanostructured surfaces (see Section 5), is particularly attractive to combat
29 infections, as it does not rely on transient drug-diffusion processes. Such processes are inherently
30 limited and subjected to depletion over time, as well as having the risk of promoting antimicrobial
31 resistance.
32
33
34
35

36
37 The co-immobilization of peptides has been widely explored to improve the osteoconductive and
38 osteoinductive properties of biomaterials.^[35] This strategy takes advantage of the well-defined
39 structure, ease of synthesis and good stability of short peptides, but improves their often moderate to
40 low bioactivity and specificity, better recapitulating the complex microenvironment of bone ECM. The
41 combination of peptide motifs has proven useful to e.g. synergize the binding towards integrin $\alpha 5\beta 1$
42 (RGD + PHSRN),^[78,79,169] improve osteoblast functions via integrin and proteoglycan binding (RGD
43 + KRSR/FHRRIKA)^[80,170,171] or trigger integrin and growth factor signaling (RGD + BMP-derived
44 peptides).^[172,173] These approaches will not be covered here, but are described in detail in the
45 literature.^[35,174]
46
47
48
49
50
51
52

53
54 The combination of cell adhesive sequences with AMPs offers excellent opportunities to develop
55 multifunctional biomaterials. It is important to note that AMPs display high potency against a broad
56 spectrum of bacteria. Moreover, the mechanism of action of AMPs (i.e. interaction with bacterial
57 membranes) appears to have a lower propensity to develop antibacterial resistance compared to
58
59
60
61
62
63
64
65

1 conventional antibiotics.^[175,176,177,178] Following this rationale, the functionalization of Ti with an
2 equimolar mixture of an RGD peptide and the AMP HHC36 inhibited the attachment of
3 *Staphylococcus aureus* and *Escherichia coli* while improving bone marrow stromal cell (BMSC)
4 adhesion.^[179] Although the authors implemented a *click chemistry*-based methodology to modify the
5 proportion of peptide grafting, controlling the concentration, ratio, and spatial organization of peptide
6 mixtures upon binding to a surface is a challenging task and not always possible. To address that, we
7 developed a peptidic branched platform with the capacity to simultaneously present two peptide
8 sequences in a chemically controlled fashion.^[78,79] Using this platform we recently combined the RGD
9 sequence with LF1-11, an AMP derived from lactoferrin that showed excellent antibacterial properties
10 on Ti surfaces.^[180,181] Such approach very effectively improved OB adhesion, proliferation and
11 mineralization, and inhibited *Staphylococcus aureus* and *Streptococcus sanguinis* attachment and
12 biofilm progression (Figure 5).^[182] Importantly, the bifunctional molecule was also effective in a co-
13 culture scenario in which the surfaces were exposed to bacterial suspensions (pre-infective condition)
14 for 2h before seeding OB-like cells. On non-functionalized surfaces the presence of bacteria drastically
15 inhibited cell attachment. In contrast, on the surfaces coated with the RGD/LF1-11 platform, normal
16 cell adhesion and viability was preserved. SEM analysis further revealed that in such a competitive
17 scenario, bacteria directly interfered with OBs (e.g. by surrounding and covering them), preventing
18 eukaryotic cells from attaching and adequately spreading. The multifunctional coating, through its dual
19 cell adhesive and antibacterial effect, proved useful to overcome the deleterious effects of initial
20 bacterial adherence. These data support the concept of the “race for the surface”^[14,38] and indicates that
21 rather than a competition cells actually “fight for the surface”.

22 Although this strategy has potential to develop anti-infective coatings, it should be emphasized that
23 surviving bacteria, even very low numbers, might be capable of proliferating on the implant surfaces,
24 initiating the formation of new biofilms. Moreover, bacterial debris and proteins from the extracellular
25 environment may serve as new anchoring points for other colonizers.^[183] To solve this, cell adhesive
26 and antibacterial peptides can be combined together with anti-adhesive polymer coatings to confer
27 biomaterials with a trifunctional potential (cell adhesive, bacterial repellent/bacteriostatic and
28 bactericidal). We recently followed this approach (Figure 6), combining PEG coatings
29 electrodeposited onto Ti surfaces with the aforementioned RGD/LF1-11 platform, which was
30 covalently attached to the PEG layers using a maleimide crosslinker.^[184] As expected, PEG coatings
31 inhibited protein adsorption and cell (both bacteria and OB-like cells) adhesion. However, the presence
32 of the RGD sequence efficiently rescued cell adhesion, while the AMP increased the antibacterial
33 potential of the coatings, reaching values of *Streptococcus sanguinis* adhesion below 0.2% (Table 2
34
35
36
37
38
39
40
41
42
43
44
45
46
47
48
49
50
51
52
53
54
55
56
57
58
59
60
61
62
63
64
65

1 and Figure 6). In another example, the triblock copolymer Pluronic F127 (PEG-polypropylene glycol-
2 PEG) (PF127) was functionalized with either RGD or an AMP to coat the biomaterial surfaces.^[185] In
3 detail, surfaces were coated with different mixtures of PF127, PF127-RGD and PF127-AMP. By
4 tuning the proportion of these polymers, antibacterial potential against *Staphylococcus aureus*,
5 *Staphylococcus epidermidis*, and *Pseudomonas aeruginosa*, or improved FB adhesion could be
6 obtained.
7
8
9

10
11 An alternative approach would be the combination of AMPs with GFs. In this regard, Yüksel et al.
12 recently described a bilayer of PLGA membranes with antibacterial and bioactive properties.^[186] The
13 dual function was achieved by covalently immobilizing the AMP magainin II within one of the layers,
14 and incorporating epidermal growth factor (EGF) in the other layer. This approach reduced the
15 adhesion of *Escherichia coli* and *Staphylococcus aureus* and supported FB adhesion. This strategy
16 opens the way to combine AMPs with other GFs (e.g. BMPs) or osteogenic peptides. Particularly
17 interesting would be the co-immobilization of AMPs with BMP-derived peptides,^[187,188] as this
18 strategy would allow for an osteogenic effect at the implantation site, reducing the risk of an
19 uncontrolled release of GFs. However, while RGD has been co-immobilized with peptides derived
20 from BMP-2^[172] or BMP-7,^[173] showing enhanced osteogenic differentiation of stem cells, the
21 combination of BMP-mimetics with AMPs remains to be explored. Another approach that deserves
22 further investigation is to integrate dual functions within one single biomolecule. Bronk *et al.*
23 engineered a collagen-mimetic molecule that upon immobilization on Ti enhanced OB-like cell
24 adhesion and differentiation, and prevented *Staphylococcus aureus* and *Staphylococcus epidermidis*
25 colonization.^[189] Godoy-Gallardo *et al.* reported a simple but effective multifunctional strategy by
26 grafting triethoxysilypropyl succinic anhydride (TESPSA) silane on Ti. Silanes have been widely used
27 as crosslinker to attach bioactive peptide sequences; however, in this study, the silane alone enhanced
28 the expression of osteogenic markers on OB-like cells, decreased the adhesion of *Streptococcus*
29 *sanguinis* and *Lactobacillus salivarius*, and supported FB adhesion in a co-culture competitive setting
30 in the presence of bacteria.^[190] Yuran et al. recently reported a minimalistic bifunctional peptide
31 combining the RGD sequence with two units of fluorinated phenylalanine (Phe(4-F)), which promoted
32 peptide self-assembly into cell adhesive and bacterial resistant coatings.^[191] The amino acid 3,4-
33 dihydroxyphenylalanine (DOPA) was used as anchoring unit to bind the peptide to Ti surfaces (Table
34 2).
35
36
37
38
39
40
41
42
43
44
45
46
47
48
49
50
51
52
53
54
55
56
57
58
59
60
61
62
63
64
65

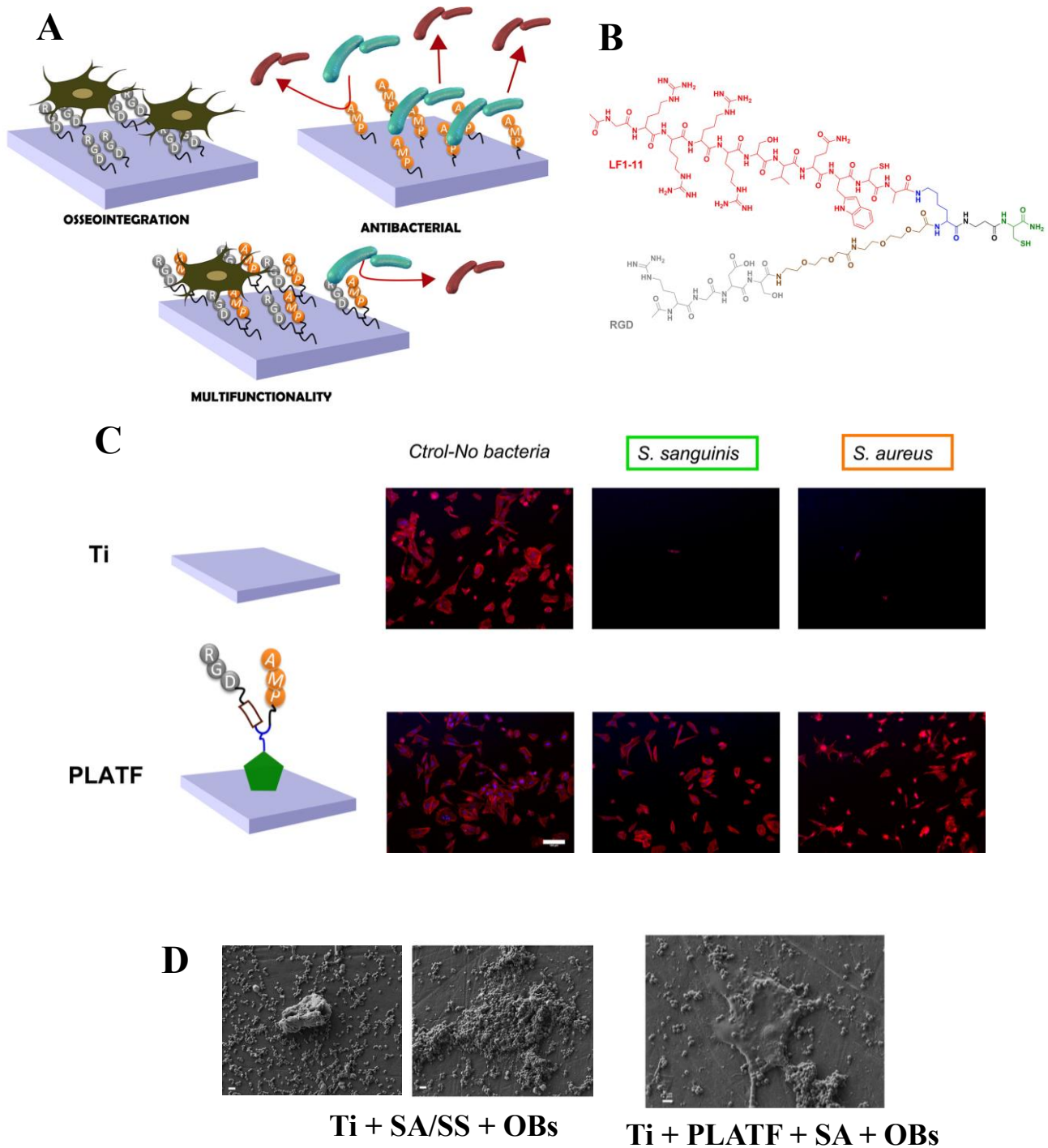


Figure 5: A) Classical approaches tend to functionalize surfaces with either cell adhesive or antibacterial peptides, but ignore a combined effect. Using a peptidic platform both activities can be simultaneously exploited on the biomaterial surface; B) Chemical structure of the multifunctional platform; C) Immunostaining of actin fibers on cell-bacteria co-culture studies. Pre-incubation of Ti surfaces with bacteria (*S. sanguinis* or *S. aureus*) inhibits the adhesion of OB-like cells (upper row); functionalizing the surfaces with the platform restores cell adhesion to normal levels (lower row); D) SEM analysis of OB-bacteria interactions. In the absence of the platform bacteria surround cells and block their spreading. SS: *S. sanguinis*; SA: *S. aureus*. **Reproduced (adapted) with permission.**^[182] Copyright 2017, American Chemical Society.

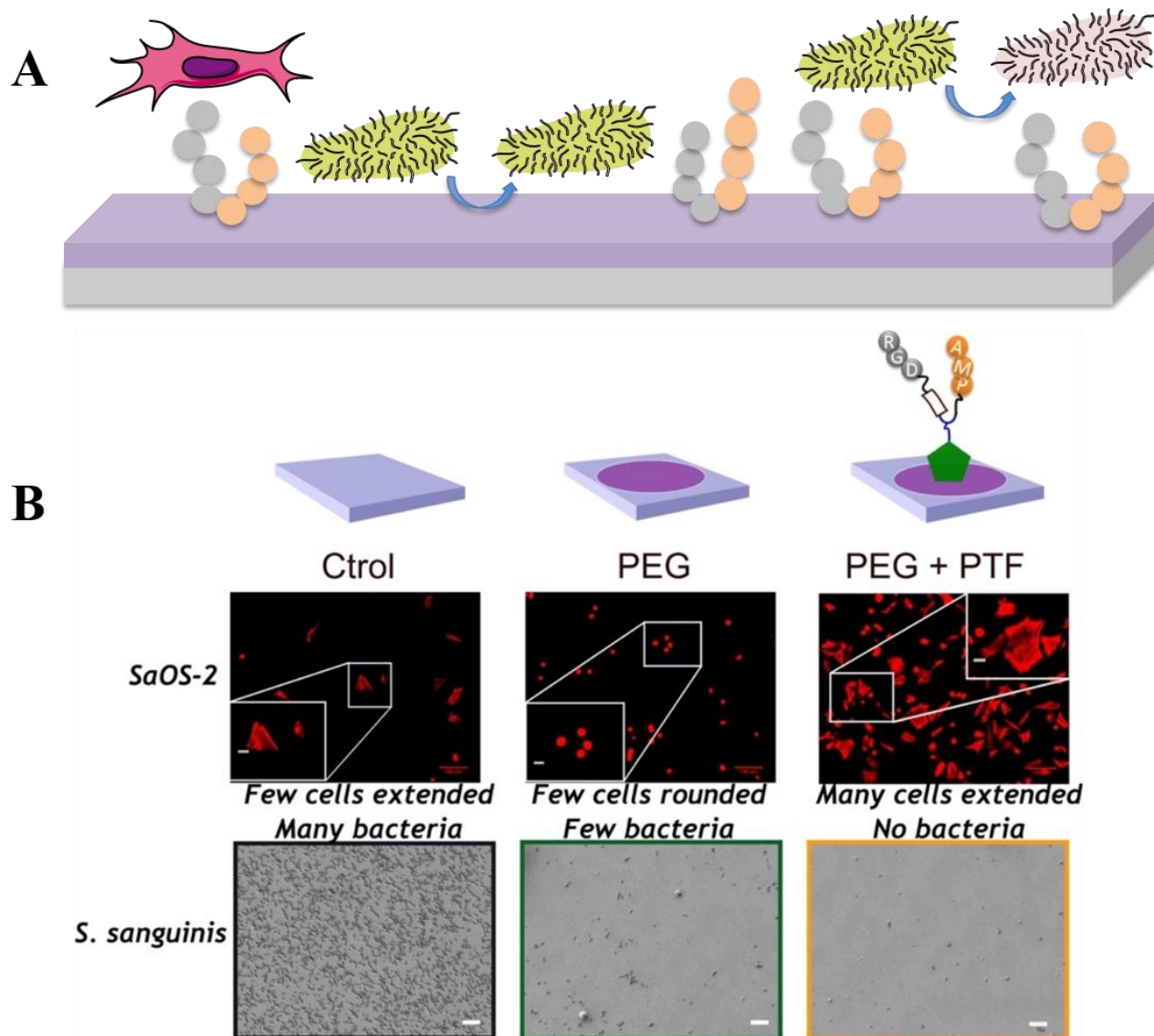


Figure 6: A) Trifunctional strategy: i) a repellent coating (e.g. PEG) prevents bacterial attachment; ii) a cell adhesive sequence (e.g. RGD) supports eukaryotic cell adhesion; and iii) a bactericidal molecule (e.g. AMP) kills adhering bacteria; B) Combining the low fouling potential of PEG with a cell adhesive/bactericidal platform (RGD + LF1-11) efficiently supports OB-like cell adhesion but totally suppresses the adhesion of *S. sanguinis*. Figure 6B is reproduced with permission.^[184] Copyright 2018, Elsevier.

Table 1. Selection of representative examples of multifunctional approaches on biomaterials

Strategy	Biofunctional elements	Substrate + coatings (immobilization method) ^[a]	Main biological effects ^[b]	References
Functionalized anti-adhesive polymer	PEG + RGD	Ti + PLL-g-PEG (electrostatic adsorption) + RGD (vinyl sulfone-thiol)	↓ <i>S. aureus</i> adhesion; Cell adhesion not studied	[106]
	PEG + RGD	Ti + PLL-g-PEG (electrostatic adsorption) + RGD (vinyl sulfone-thiol)	↓ Bacterial adhesion (several strains); Cell adhesion not studied	[107]
	PEG + RGD	Ti + PLL-g-PEG (electrostatic adsorption) + RGD (vinyl sulfone-thiol)	↓ <i>S. epidermidis</i> adhesion; ↑ OB-like adhesion	[108]
	PEG + RGD	Ti + PEG (several methods) + RGD (physisorption)	↓ <i>S. sanguinis</i> and <i>L. salivarius</i> adhesion; ↑ FB adhesion	[109]
	Dextran + BMP-2	Ti6Al4V-dopamine + dextran (reductive amination) + BMP-2 (reductive amination)	↓ <i>S. aureus</i> and <i>S. epidermidis</i> ; ↑ OB response	[110]
	PMAA + silk sericin	Ti + PMAA (silanization + SI-ATRP) + silk sericin (carbodiimide chemistry)	↓ <i>S. aureus</i> and <i>S. epidermidis</i> adhesion; ↑ OB response	[111]
	HA + VEGF	Ti + catechol-HA (direct chemisorption) + VEGF (carbodiimide chemistry)	↓ <i>S. aureus</i> adhesion; ↑ OB response	[112]
Functionalized bactericidal polymer	CM-CH + VEGF	Ti-dopamine + CM-CH (carbodiimide chemistry) + VEGF (carbodiimide chemistry)	↓ <i>S. aureus</i> adhesion; ↑ OB response	[112]
	HA/CH + RGD	Ti + HA/CH (PEMs electrostatic adsorption) + RGD (carbodiimide chemistry)	↓ <i>S. aureus</i> adhesion; ↑ OB response	[121]
	CH + RGD	Ti-dopamine + CH (glutaraldehyde crosslinking) + RGD (carbodiimide chemistry)	↓ <i>S. aureus</i> and <i>S. epidermidis</i> adhesion; ↑ OB response	[122]
	CM-CH + BMP-2	Ti6Al4V-dopamine + CM-CH (carbodiimide chemistry) + BMP-2 (carbodiimide chemistry)	↓ <i>S. aureus</i> and <i>S. epidermidis</i> adhesion; ↑ OB and MSC response	[123]
	CM-CH + ALP	Ti-dopamine + CM-CH (carbodiimide chemistry) + ALP (carbodiimide chemistry)	↓ <i>S. epidermidis</i> adhesion; ↑ OB, MSC and ADSC osteogenic differentiation	[125]
	CH/PAA + Ga	Ti + PAA (electropolymerization) + CH-Ga (electrochemical deposition)	↓ <i>E. coli</i> and <i>S. epidermidis</i> viability; OB-like adhesion supported and ↑ BMP-2 expression	[126]

Osteoconductive /osteoinductive surface loaded w/ antibacterial agents	TNT + Ag	Ti > TNT (anodization) + Ag (electrodeposition)	↓ <i>P. aeruginosa</i> adhesion; Biocompatible for OBs	[132]
	TNT + Ag ₂ O NPs	Ti > TNT-Ag ₂ O (TiAg magnetron sputtering and anodization)	↓ <i>S. aureus</i> and <i>E. coli</i> ; OB-like response not influenced compared to TNTs	[133]
	TNT + Zn	Ti > TNT (anodization) + Zn (hydrothermal treatment)	↓ <i>S. aureus</i> adhesion and proliferation; ↑ OB-like response; ↑ Bone formation <i>in vivo</i>	[135]
	TNT + gentamicin + CH/PLGA	Ti > TNT (anodization) + gentamicin (drop casting) + CH/PLGA (dip coating)	↓ <i>S. epidermidis</i> viability; ↑ OB-like response	[138]
	HAp + Ag ₂ O + SrO	Ti + HAp/Ag ₂ O/SrO (plasma spray)	↓ <i>P. aeruginosa</i> viability; ↑ OB-like response for HAp + Ag/Sr compared to HAp	[150]
	CaP + HHC36	Ti + HAp (electrolyte deposition) + HHC36 (physical adsorption)	↓ <i>P. aeruginosa</i> and <i>S. aureus</i> viability; ↑ OB-like cell adhesion; ↑ Bone formation <i>in vivo</i>	[154]
	cRGD + roxithromycin	Ti + RGD-NPs/roxithromycin (silanization; roxithromycin is loaded by emulsification)	↓ <i>S. sanguinis</i> adhesion; ↑ OB-like response	[164]
	BMP-2 + vancomycin	Ti + BNP/BMP-2 + BNP/vancomycin (layer-by-layer adsorption; drugs are loaded by a desolvation method)	↓ <i>S. epidermidis</i> growth; ↑ BMSC response	[167]
Immobilized peptides	RGD + HHC36	Ti + RGD/HHC36 (silanization + click chemistry)	↓ <i>S. aureus</i> and <i>E. coli</i> adhesion; ↑ BMSC adhesion	[179]
	RGD + LF1-11	Ti + RGD/LF1-11 (silanization)	↓ <i>S. aureus</i> and <i>S. sanguinis</i> ; ↑ OB-like response	[182]
	PEG + RGD + LF1-11	Ti + PEG (electrodeposition) + RGD/LF1-11 (maleimide-thiol chemistry)	↓ <i>S. sanguinis</i> ; ↑ OB-like response	[184]
	PF127 + RGD + AMP	Silicon + PF127/PF127-RGD/PF127-AMP (physical adsorption)	↓ <i>S. aureus</i> , <i>S. epidermidis</i> and <i>P. aeruginosa</i> adhesion; ↑ FB adhesion	[185]
	EGF + magainin II	PLGA + EGF (physical entrapment) + magainin II (carbodiimide chemistry)	↓ <i>S. aureus</i> and <i>E. coli</i> adhesion; ↑ FB adhesion	[186]
	Collagen-mimetic	Ti + collagen-mimetic (physisorption)	↓ <i>S. aureus</i> and <i>S. epidermidis</i> adhesion; ↑ OB-like adhesion and differentiation	[189]
	TESPSA silane	Ti + TESPSA (silanization)	↓ <i>S. sanguinis</i> and <i>L. salivarius</i> adhesion; ↑ OB-like differentiation; ↑ FB adhesion	[190]
	RGD + Phe(4-F)	Ti + DOPA-peptide (chemisorption)	↓ <i>E. coli</i> adhesion; ↑ OB-like adhesion	[191]

15
16
17
18
19
20
21
22
23
24
25
26
27
28
29
30
31
32
33
34
35
36
37
38
39
40
41
42
43
44
45
46
47
48
49
50
51
52
53
54
55
56
57
58
59
60
61
62
63
64
65

[a] “Substrate” refers to the material used, and “coating” to the combination of chemical entities that exhibit multiple biological activity; the methods used to immobilize the coatings are described in brackets.

[b] Only the main biological effects are highlighted. Reduced bacterial adhesion commonly indicates a reduction in bacterial cell numbers compared to controls. Improved cell response usually refers to increased values of cell adhesion, proliferation and differentiation compared to controls. Detailed data can be found in the corresponding references.

Abbreviations used: ADSC = adipose-derived stem cell; BMSC = bone marrow stromal cell; BMP = bone morphogenetic protein; **BNP = BSA-based nanoparticle**; CH = chitosan; CM-CH = carboxymethyl chitosan; cRGD = cyclic RGD; **DOPA = 3,4-dihydroxyphenylalanine**; FB = fibroblast; HA = hyaluronic acid; HHC36 peptide = (KRWWKWWRR); MSC = mesenchymal stem cell; NP = nanoparticle; OB = osteoblast; PAA = poly(acrylic acid); PEG = poly(ethylene glycol); PEMs = polyelectrolyte multilayers; **Phe(4-F) = fluorinated phenylalanine**; PLL-g-PEG = poly-L-lysine-graft-poly(ethylene glycol); PMAA = poly(methacrylic acid); SI-ATRP = surface initiated atom transfer radical polymerization; VEGF = vascular endothelial growth factor;

Bacterial strains: *Escherichia coli* = *E. coli*; *Lactobacillus salivarius* = *L. salivarius*; *Pseudomonas aeruginosa* = *P. aeruginosa*; *Staphylococcus aureus* = *S. aureus*; *Staphylococcus epidermidis* = *S. epidermidis*; *Streptococcus sanguinis* = *S. sanguinis*; *Streptococcus mutans* = *S. mutans*.

4. Osteogenic nanotopographies

1
2 We have already discussed that implant osteointegration can be enhanced by physical and
3 chemical methods. While physical modifications (i.e. surface roughness) improve implant
4 functionality by increasing its micromechanical retention with bone, chemical coatings such as
5 integrin-binding molecules or CaP have been described to promote osteogenesis from
6 mesenchymal stem cells (MSCs). While roughness is undoubtedly useful, it is hard to dissect
7 effects as surfaces with two similar Ra values can appear very different and so could potentially
8 have different effects on cells. This section of the review will focus on cell response to defined
9 nanotopography with particular consideration on nanotopographically-directed osteogenesis.
10 We note that roughness based approaches are being developed – most notably for orthopedic
11 application (see Section 2.1). These are not a focus of this review, but excellent reviews are
12 available.^[192,193]

13
14 The ability of surface topography to guide cells has been known for over 100 years,^[194] with
15 the term ‘contact guidance’ becoming used in the 1950/60s.^[195,196] In the 1980s, understanding
16 of the cell-topographical interaction at the microscale started to become elucidated thanks to
17 microfabrication techniques such as photolithography and wet/dry etch.^[197,198] This
18 proliferation of biological data revealed that all cell types tested responded to
19 microtopographical features.^[199,200,201,202,203,204,205] As semiconductor technology advanced to
20 help develop faster computer microchips, the study of nanotopographical-cell interactions
21 became possible with first indications of the cells’ ability to contact guide to nanopatterns
22 shown using substrates derived from laser holographical lithography.^[206] By the turn of the 21st
23 century, both top-down (lithographical, e.g. electron beam lithography, colloidal
24 lithography^[207,208,209]) and bottom up (e.g. polymer phase separation, block co-polymer
25 separation, etc.^[210,211,212,213]) approaches were becoming available to cell biologists. These
26 substrates allowed development of understanding that cells could respond to features where all
27 features were nanoscale;^[214] soon it was understood that a broad range of cells could respond
28 to nanoscale features^[215] – even platelets.^[216]

29
30 Considering controlled topography, top-down techniques such as electron beam lithography
31 (EBL) allow patterning for cell experimentation with features down to 10 nm in size.^[217]
32 Moving from cell-scale to clinical-scale may, however, be challenging for such techniques.

33
34 In contrast, bottom-up techniques such as polymer phase separation,^[211] colloidal
35 lithography,^[218] block co-polymer lithography^[219] and micelle lithography^[220] where larger
36 areas can be fabricated more simply – but with some loss of the resolution that EBL can offer

1
2
3
4
5
6
7
8
9
10
11
12
13
14
15
16
17
18
19
20
21
22
23
24
25
26
27
28
29
30
31
32
33
34
35
36
37
38
39
40
41
42
43
44
45
46
47
48
49
50
51
52
53
54
55
56
57
58
59
60
61
62
63
64
65

– are gaining popularity. However, for bone formation perhaps this is not so important. A study using EBL to fabricate nanopits with 120 nm diameter, 100 nm depth and 300 nm-center-to-center positioning in a square pattern showed that MSCs did not form osteoblasts when the features were precisely placed (in fact a later study showed enhanced MSC self-renewal^[221]) – rather osteoblast specific differentiation was only observed when the features were slightly offset (by up to ± 50 nm from the center positioning) (Figure 7A).^[222] It is thus noteworthy that block co-polymer micelles can now be fabricated almost to the scale that EBL has been used to generate controlled nanodisorder, i.e. with ± 50 nm feature offsets known to drive cell function.^[223] Copies (via nickel shims) of phase separated nanosurfaces and colloidal nanosurfaces in bio-polymers (polymethylmethacrylate and polycaprolactone) have now been shown to influence MSC growth *in vitro*.^[224] Further, such bottom-up methodologies have been used to generate masks for anodization of e.g. Ti implant materials to enhance osteogenesis.^[225,226,227,228]

Moving into 3D is challenging for lithographical and demixing processes due to their 2D natures. Interestingly for tissue engineering, polymer demixing can be performed inside 3D constructs such as tubes^[229] and, indeed, influence MSC growth.^[230] Tube-like structures are typical in bone e.g. Haversian and Volkman’s canals (the osteon system). A further major development towards 3D is a topographical approach with the potential to incorporate ultra-precise (e.g. lithographical) nanotopographical fabrication.^[231] In this system, a biodegradable polymer (e.g. polycaprolactone) was embossed between two micron or nanopatterned surfaces. Included in the design were spacing posts (approx. 50 μm high) to allow perfusion of media and oxygen during pre-conditioning. The embossed sheet was rolled to form a larger construct and seeded with cells prior to pre-conditioning *in vitro*. Also, ‘car-park’ assemblies have been made using osteogenic micropatterns embossed onto polymeric sheets that incorporate large spacers to separate layers of the ‘car-park’;^[232] embossing of osteogenic nanotopographies in this system is easily envisaged.

If we consider mechanism of cellular response, cell adhesions are very sensitive to nanoscale features, being able to form filopodia in response to topographies down to 10 nm in height^[233] but, further, being seen to have to have ‘nanopodial’ interactions down to 8 nm in height.^[234] At the microscale, contact guidance by features of similar scale to the cells themselves is easy to envisage (i.e. they have no choice). At the nanoscale, however, subcellular features, i.e. adhesions, must reorganize to guide cells. As adhesive proteins encounter a nanoscale cue (e.g. a nanogroove or a fibronectin line) - an order of magnitude smaller than the cell, but on a similar

1 scale to filopodia and integrin receptors - the adhesions will elongate along the cue and this, in
2 turn, will drive actin alignment in the direction of the cues.^[235] This will align the cell literally,
3 and metaphorically, from the bottom-up (in fact, this is a first step for large scale tissue
4 organization during development).
5

6
7 In the context of this review, particularly studied has been MSC to osteoblast (bone forming
8 progeny) differentiation. A range of nanoscale topographies from nanodisordered surfaces,^[222]
9 to biomimetic helical structures with collagen-like 63 nm periodicity^[236] has been demonstrated
10 to induce osteogenesis (Figure 7B).
11
12

13
14 At the cell-material interface, cell adhesion formation has been widely studied and is considered
15 important in defining MSC to osteoblast differentiation. When observing MSC differentiation
16 to bone, it is not the number of adhesions that a cell can form *per se* that is important for bone
17 production, rather the size of the adhesions. Studying MSC adhesion size during osteogenesis
18 shows that larger adhesions form.^[222] In addition, it has been shown using RGD functionalized
19 gold nanopatterns that a slight disorder significantly enhances MSC adhesion.^[220] It has been
20 seen that disorder can increase adhesion through bringing groups of adhesive points closer
21 together, into a critical 70 nm range^[237] to facilitate gathering of integrins into focal adhesions
22 and thus facilitate integrin gathering. Also, MSCs cultured on osteogenic nanopatterns have
23 been indicated to express endogenous vitronectin over fibronectin.^[238] Vitronectin may be
24 important, as it allows better bridging between integrin clusters via intracellular adhesion
25 proteins such as vinculin and talin.^[239] Efficient bridging will allow cells to form larger, more
26 mature adhesions, over discontinuities such as nanopits.
27
28
29
30
31
32
33
34
35
36
37
38
39

40 In further consideration of adhesion mechanism, the formation of “super-mature” adhesions
41 (SMAs)^[240] (> 5 μm long) is important for stabilizing the large osteoblast morphology and
42 resultant bone formation. It is likely that such super-mature adhesions are stabilized/scaffolded
43 by proteins such as RACK1,^[241,242] allowing increased levels of intracellular tension,^[243,244]
44 mediated by RhoA Kinase (ROCK), important to MSC fate.^[245,246,247]
45
46
47
48
49
50
51
52
53
54
55
56
57
58
59
60
61
62
63
64
65

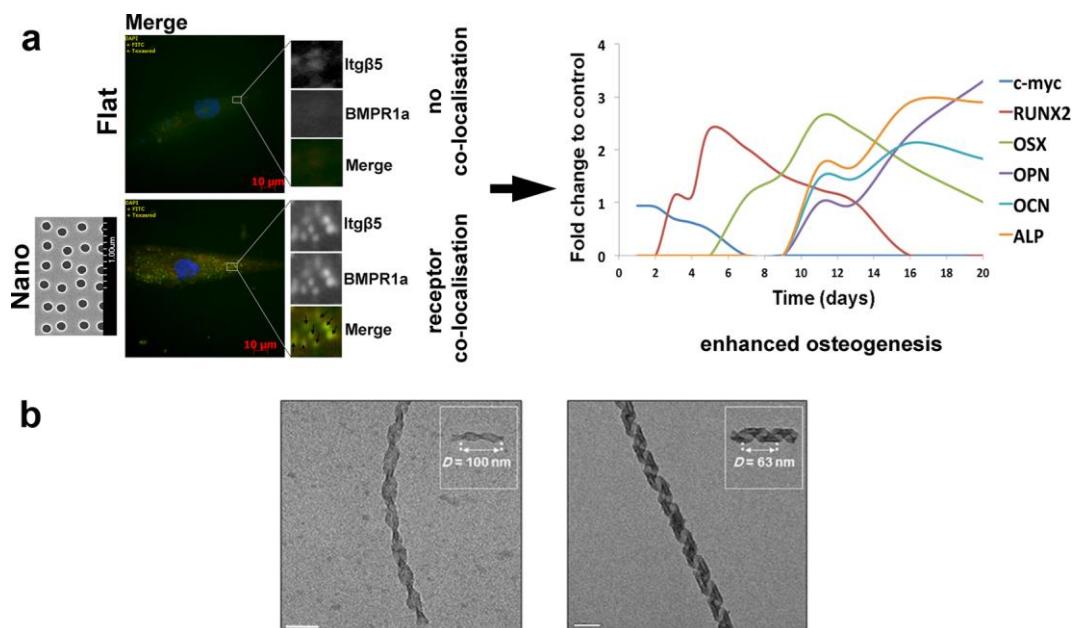


Figure 7. Nanoscale topographical control of MSC differentiation. (A) MSCs respond to nanoscale disorder. Using electron beam lithography to fabricate arrays of nanopits (120 nm diameter, 100 nm deep) in a square array (SQ, 300 nm center-center pitch) with up to ± 50 nm offset from the center square position (nano), increased adhesion and adhesion co-localization of integrin (here integrin beta 5 is stained) and the BMP2 receptor (here BMPR1a is stained) and this drives MSC osteogenic progression, as demonstrated by expression patterns of the osteogenic genes RUNX2 (runt related transcription factor 2), osterix (OSX), osteopontin (OPN), osteocalcin (OCN) and alkaline phosphatase (ALP). Reproduced (adapted) under the terms of the Creative Commons Attribution 4.0 International license (CC BY 4.0) [238] Copyright 2014, American Chemical Society. (B) Synthetic collagen banding patterns with 100 nm repeat (non-physiological) and 63 nm repeat (physiological); MSCs are stimulated to undergo osteogenesis on the physiological pattern, but not the non-physiological pattern. Reproduced (adapted) with permission. [236] Copyright 2013, American Chemical Society.

5. Antimicrobial nanotopographies

We have seen in the previous sections that current strategies to combat biomaterials-associated infections are largely reliant upon chemical means i.e. use of polymers (or surface functional groups) to prevent protein adsorption and inhibit bacterial adhesion, or coatings that release chemical agents such as antibiotics, silver ions or quaternary ammonium salts into the surrounding microenvironment. A critical limitation of these chemistry-based strategies is that they are transient because leaching of antimicrobial agents is limited and subject to depletion over time. Dwindling antibiotic concentration and/or prolonged bacterial colonization of materials may also inadvertently promote development and spread of antimicrobial resistance. A physical approach, such as topography, could potentially overcome the above problems and offers completely new and alternative solutions to biomaterial infections.

5.1 Anti-biofouling nanotopographies

1
2 Surface topography has been known to alter bacterial adhesion and biofilm formation. It has
3
4 become evident that surface hydrophobicity/hydrophilicity and effective contact area are two
5
6 key factors that are responsible for the different bacterial adhesive behavior on surfaces. A well-
7
8 known example is the superhydrophobic ‘lotus effect’, which is the result of a combination of
9
10 hydrophobic chemistry (wax) and the hierarchical and multiscale surface structure, i.e.,
11
12 nanostructures on microstructures. The hydrophobic epicuticle layer, with high density of nano-
13
14 featured wax crystalloids, covers micro-featured convex surface structures, creating a surface
15
16 with very high contact angle (ca. 161°).^[248] It was found that when the surface of a lotus leaf
17
18 was dipped in ethanol to remove the wax, the contact angle of a water drop decreased
19
20 dramatically from ca. 161° to 122° , and the water droplet was pinned to the surface.^[249] This
21
22 intrinsic hydrophobicity of the surface principally originated from the pure hierarchy of
23
24 multiscale structures, similar to that observed on the surface of a rose petal. The lotus effect
25
26 requires air to become “trapped” between the nanostructures on the surface, i.e. the Cassie and
27
28 Baxter state, while the rose petal effect allows the liquid film to impregnate the micro/nano
29
30 topographies, i.e. the Wenzel state, because the non-waxy petal surface has a good wetting
31
32 characteristics with water. Many plant leave surfaces with micro/nano-topographies, e.g. rice
33
34 and taro, have been shown to be able to control the bacterial fouling and biofilm
35
36 formation.^[250,251] Inspired by nature, various nanoengineered surfaces have been investigated
37
38 in terms of their surface hydrophobicity/hydrophilicity and nanotopography. Hizal et al.^[252]
39
40 reported two nanostructured superhydrophobic surfaces with extremely low bacterial adhesion
41
42 under dynamic flow condition. Both 2D nanoporous surface and 3D nanopillared surface
43
44 showed a significant reduction in adhesion for *Staphylococcus aureus* and *Escherichia coli*,
45
46 which was more pronounced for the hydrophobic surface treated with a Teflon coating (Figure
47
48 8). This was attributed to a decreased contact area for the 2D porous surface and effective air
49
50 entrapment in 3D nanopillars. The bacterial adhesion force on these nanoengineered surfaces
51
52 was reduced as measured by atomic force microscopy (AFM). Similar anti-fouling effects were
53
54 observed on hydrophilic TiO_2 nanopillars^[253] or nanotubes.^[254] The nanofeature dimensions e.g.
55
56 nanopillar diameter, height and spacing affected the bacterial adhesion due to the change of
57
58 effective contact area.^[255,256] Strong bacterial repelling has also been reported on highly ordered
59
60 alumina nanoporous surfaces^[257] and polymer (PLGA) nanopit surfaces with pore sizes ranging
61
62 from 200 to 500 nm.^[258] This contact-area-reducing approach has been attempted in real
63
64 medical applications. Serrano et al.^[259] reported oxygen plasma treated sutures with lamellae
65
66 voids with feature size \leq bacteria size. The results showed that bacterial attachment was

decreased with reduced surface contact area and effective prevention of biofilm formation was achieved in absorbable sutures with top area fractions below 30% presenting lamellae with 200-500 nm thickness and several microns in length, separated by 1-2 μm voids.

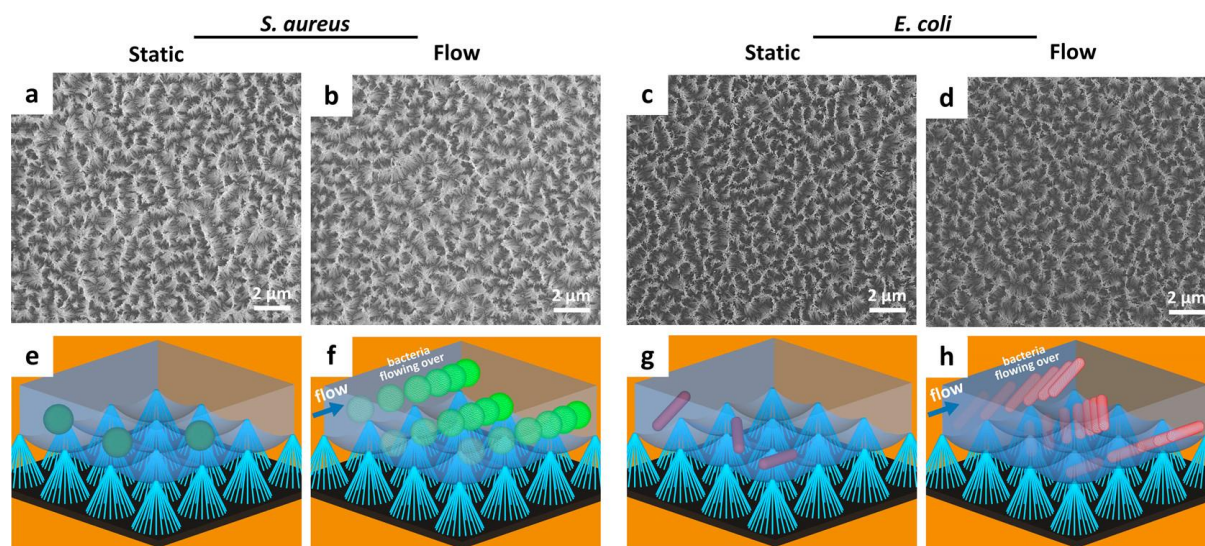


Figure 8. FE-SEM images (a–d) and schematics (e–h) representing the bacterial adhesion on hydrophobic nanopillared surfaces. In panels e and g, the schematics represent the bacteria are floating over the entrapped air layer under static conditions. In panels f and h, the schematics represent the bacteria being washed off under flow. Reproduced with permission.^[252] Copyright 2017, American Chemical Society.

5.2 Bactericidal nanotopographies

Bactericidal nanotopographies have not been reported until recently, although bactericidal nanostructures in the form of suspended colloids were investigated much earlier. For example, Liu et al. reported that the single-walled carbon nanotubes (SWCNTs) in a suspension are bactericidal upon contact with bacteria. They found that the sharpness and concentration of the SWCNTs coupled to mechanical shaking of the SWCNT suspension could enhance the bacteria-killing performance. They described these SWCNTs as ‘nano darts’ which were able to physically pierce the bacterial cells.^[260]

Ivanova et al. first reported bactericidal nanotopographies on cicada (*Psaltoda claripennis*) wings. When culturing *Pseudomonas aeruginosa* cells on *Psaltoda claripennis* wings, which comprised 200 nm tall nanopillars (or nanocones) with a diameter of 100 nm at the base and 60 nm at the cap, and spaced 170 nm apart from center to center, it was noted that the bacterium died.^[261] They postulated that cell death was caused purely by the mechanical rupturing of bacterial cell walls. A biophysical model has been developed to explain the mechano-

1 bactericidal action of the cicada wings.^[262] Kelleher *et al.* tested three different cicada wings
2 (Megapomponia intermedia, Ayuthia spectabile and Cryptotympana aguila).^[263] They found a
3 strong correlation between the bactericidal properties of the wings and the scale of the
4 nanotopographies present on the different wing surfaces. Sharper and more densely packed
5 nanopillars on Megapomponia intermedia wings killed more bacteria, probably by inducing a
6 greater strain on the bacterial cell walls. Subsequently, more naturally occurring bactericidal
7 surfaces have been reported.^[264,265] They include nanopillars on the dragonfly wing,^[266] the
8 damselfly wing,^[267] the moth eye,^[268] the rat-tailed maggot, the aquatic larva of the Drone
9 fly,^[269] and the nanotipped hairs on gecko skin.^[270]

10
11 Inspired by nature, a number of studies have since been carried out to develop bactericidal
12 nanotopographies on synthetic materials. They include silicon^[271,272,273,274] and diamond coated
13 silicon,^[275,276,277] titanium and its alloy,^[278,279,280,281,282,283,284] polymers,^[285,286,287,288] stainless
14 steel^[289] and aluminium.^[290] Table 3 lists a summary of biomimetic bactericidal surfaces on
15 various materials currently in development. Examples of some bactericidal nanotopographies
16 created on various synthetic materials are shown in Figure 9.

Table 3. Current development in biomimetic and bio-inspired bactericidal surfaces on various substrates.

Material	Surface nanotopography	Fabrication method	Bacteria studied	Ref
Silicon	Nanopillars Nanoneedles Nanowires	Reactive ion etching (RIE), metal-assisted chemical etching	<i>Pseudomonas aeruginosa</i> , <i>Staphylococcus aureus</i> and <i>Bacillus subtilis</i>	[271,272,273,274]
Diamond and diamond coated Si	Nanocones	Chemical vapour deposition (CVD) + bias assisted RIE	<i>Pseudomonas aeruginosa</i>	[275]
	Nanoneedles	RIE + CVD	<i>Pseudomonas aeruginosa</i> , <i>Escherichia coli</i> , and <i>Streptococcus gordonii</i>	[276,277]
Titanium	Nanowires	Hydrothermal growth	<i>Staphylococcus aureus</i> , <i>Staphylococcus epidermidis</i> , <i>Pseudomonas aeruginosa</i> , <i>Escherichia coli</i> , <i>Bacillus subtilis</i> , <i>Enterococcus faecalis</i> and <i>Klebsiella pneumoniae</i>	[278,279,280,281]
	Nanocolumns	Glancing angle sputter deposition	<i>Escherichia coli</i> and <i>Staphylococcus aureus</i>	[282]
	Nanopillars	Reactive ion etching	<i>Escherichia coli</i> , <i>Pseudomonas aeruginosa</i> , <i>Staphylococcus aureus</i> and <i>Mycobacterium smegmatis</i>	[283]
Ti alloy	Nanocones Nanowire	Thermal oxidation	<i>Escherichia coli</i>	[284]
Polymers	Nanopillars Nanocones	Nanoimprinting	<i>Escherichia coli</i> , <i>Pseudomona aeruginosa</i> and <i>Staphylococcus Aureus</i>	[285,286,287]
	Nanopillars Nanocones	Colloidal lithography	<i>Escherichia coli</i> and <i>Klebsiella pneumoniae</i>	[288]
Stainless steel	Nano-protruding textures	Electrochemical etching	<i>Escherichia coli</i> and <i>Staphylococcus aureus</i>	[289]
Aluminium	Micro/nano-rough surfaces	Chemical etching	<i>Escherichia coli</i> , <i>Klebsiella pneumoniae</i> and <i>Staphylococcus aureus</i>	[290]

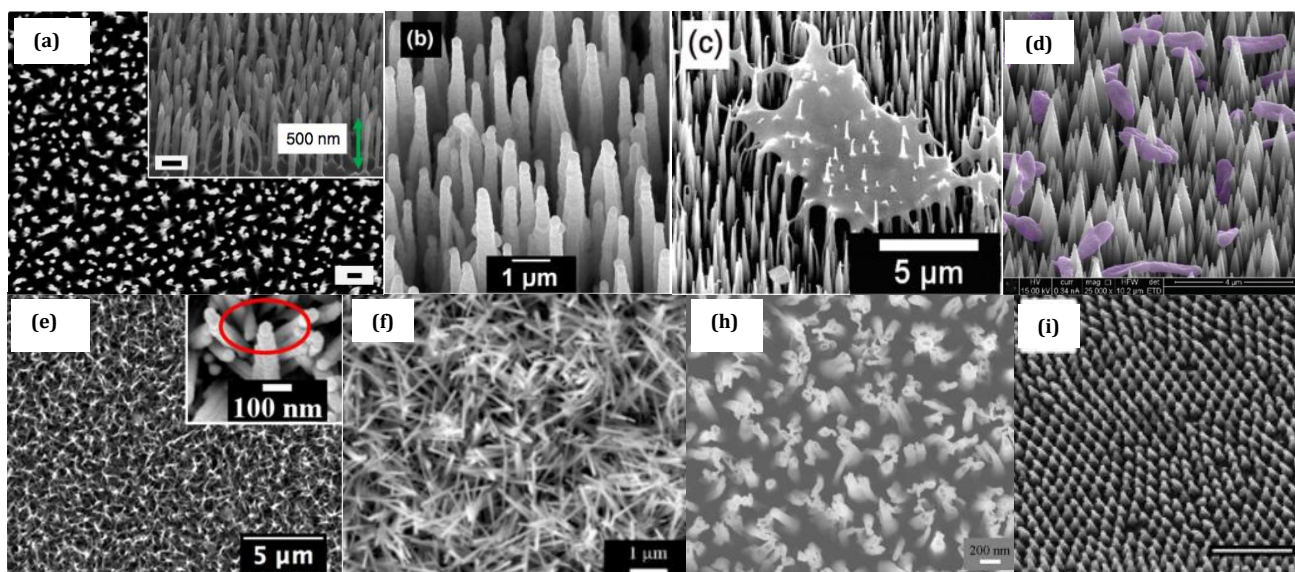


Figure 9. Examples of various synthetic bactericidal nanotopographies on different substrates.

(a) Black silicon (bSi). Reproduced with permission.^[271] Copyright 2013, Springer Nature; (b) Diamond coated bSi. Reproduced with permission.^[276] Copyright 2016, The Royal Society of Chemistry; (c) A pierced bacterium on bSi. Reproduced with permission.^[277] Copyright 2018, The Royal Society of Chemistry; (d) Diamond nanocones. Reproduced with permission.^[275] Copyright 2016, American Vacuum Society; (e) Hydrothermal TiO₂ nanowires.^[278,280] Reproduced under the terms of the Creative Commons Attribution 4.0 International license (CC BY 4.0).^[280] Copyright 2018, Springer Nature; (f) TiO₂ nanowires by thermal oxidation. Reproduced with permission.^[284] Copyright 2016, Elsevier; (g) Black titanium (bTi). Reproduced under the terms of the Creative Commons Attribution 4.0 International license (CC BY 4.0).^[283] Copyright 2017, Springer Nature; (h) PMMA nanocones. Reproduced with permission.^[285] Copyright 2015, American Vacuum Society.

Ivanova *et al.* first reported the studies of biomimetic bactericidal surfaces on synthetic materials in 2013,^[271] shortly after their discovery of bactericidal cicada wings in 2012.^[261] Nanoprotruding surfaces with high-aspect-ratio nanopillars with a diameter of 20-80 nm and a height of 500 nm were generated on silicon substrates using a reactive ion etching (RIE) method, creating ‘black silicon’ (bSi), which mimics the wings of the dragonfly *Diplacodes bipunctata*. Notably, the bSi surfaces exhibited bactericidal activity towards both Gram-positive and Gram-negative bacteria. Notably, the range and bactericidal efficacy were larger than their biological analogues (cicada and dragonfly wings). Further study indicated that the bactericidal efficacy was strongly dependent on their feature sizes. Smaller and more densely packed pillars exhibited the greatest bactericidal activity.^[273] The decrease in the nanopillar heights, nanopillar cap diameter and inter-nanopillar spacing corresponded to a subsequent decrease in the number of attached cells for both Gram-positive and -negative bacterial species.^[273]

Similar nanopillar and nanowire surfaces using different etching methods also displayed similar bactericidal activity.^[272,273,274] Susarrey-Arce *et al.* investigated the interaction and the viability

1 of bacteria of highly-oriented silicon nanowires (SiNWs) with and without functionalization.
2 They found that the bare SiNWs and SiNWs functionalized with a silane (APTES) exhibited
3 some degree of intrinsic bactericidal activity towards *Escherichia coli* and *Staphylococcus*
4 *aureus*. However, bacterial cells could still proliferate for a long time on these topographic
5 surfaces. By functionalization with chlorhexidine digluconate (CHD), the antimicrobial
6 performance was greatly enhanced because CHD released from the surface had the potential to
7 decrease the viability of both sessile and planktonic bacterial cells. They have also identified
8 two different growth modes producing distinct in-plane and out-of-plane bacterial colonies for
9 *Escherichia coli* and *Staphylococcus aureus*, respectively.^[274] However, silicon is a non-load-
10 bearing material and thus has limited application in biomedical implants.
11
12
13
14
15
16
17

18 Diamond coating using thin film technology is becoming an attractive approach for material
19 functionalization for biomedical applications due to its unique properties. It is bioinert and its
20 electrical conductivity can be tuned from insulating to near-metallic, which makes it a potential
21 candidate material for orthopedic and neural device applications.^[291] Fisher *et al.* demonstrated
22 that diamond nanocone arrays deposited on a silicon substrate via microwave plasma CVD
23 followed by bias-assisted RIE were bactericidal towards *Pseudomonas aeruginosa*.^[275] Similar
24 antimicrobial performance has also been reported for diamond coated bSi nanoneedles.^[276,277]
25 Interestingly, such a diamond coating or film could be deposited on Ti substrates, which may
26 have important medical implications, as Ti metal and its alloys are widely used materials in
27 orthopedic, dental and cardiovascular applications.
28
29
30
31
32
33
34
35
36

37 Because of the wide applications of Ti in biomedicine and the frequent biomaterials associated
38 infections, the generation of antimicrobial nanosurfaces directly on Ti substrates would be
39 desirable. Inspired by the cicada wings, Diu *et al.* first investigated bactericidal property and
40 biocompatibility of nanowires grown directly on Ti substrates using an alkaline hydrothermal
41 method.^[278] It was found that motile and Gram-negative bacteria are more susceptible to killing
42 than non-motile and Gram-positive ones. Culturing in dynamic (shaking) conditions also
43 induced more killing compared to standard static bacterial cell culture condition. It is suggested
44 that the thicker cell wall (peptidoglycan layer) found in Gram-positive cells and a lack of
45 motility in non-motile cells may be responsible for their inferior susceptibility to killing.
46
47
48
49
50
51
52
53

54 Similar works have reported on hydrothermal nanowires with various bactericidal
55 performances depending on processing and culturing conditions.^[279,280,281] Cao *et al.*
56 investigated longer-term biofilm formation of *Staphylococcus epidermidis* on spear or brush-
57 type and pocket or niche-type nanowires. Pocket-type nanowire surfaces were found to delay
58
59
60
61
62
63
64
65

1 biofilm formation up to 6 days and exhibited more recalcitrance towards *Staphylococcus*
2 *epidermidis* biofilm formation. It was believed that micro-sized pockets formed by the
3 intertwined nanowires may result in the entrapment of bacterial cells which prevented their
4 crosstalk and proliferation.^[280] The advantage of hydrothermal treatments are that they can be
5 easily applied to porous Ti substrates.^[292] Nano-flowers, rods and wires were formed in porous
6 Ti alloy scaffolds using an aqueous mixture of calcium hydroxide [Ca(OH)₂] and sodium
7 tripolyphosphate [STPP] depending on their ratios and hydrothermal conditions. Nanowire
8 surfaces exhibited bactericidal properties against *Staphylococcus aureus* and *Escherichia coli*
9 as well as osteogenesis from bone cells. Similarly, nanowire surfaces were generated on Ti
10 alloy substrates using a controlled thermal oxidation method, which also showed
11 bactericidal^[284] and osteogenic^[293] properties. Crucially, this method could be applied to porous
12 and complex shaped Ti substrates, which paves the way to develop cell-instructive
13 nanotopographies for implant applications.

14 Other fabrication methods have been investigated to produce nanostructured surfaces on Ti
15 substrates. Sengstock *et al.* reported Ti nanocolumnar structures produced using a glancing
16 angle sputter deposition (GLAD) technique. It was again observed that there was more killing
17 of Gram-negative rod-shaped *Escherichia coli* than the Gram-positive sphere-shaped
18 *Staphylococcus aureus*. Apart from their cell wall differences discussed before, their different
19 cell viability on the nanocolumnar structures may also be resulted from their difference in the
20 structural process of cell division. Rod-shaped *Escherichia coli* bacteria multiply by elongating
21 which requires an in-plane movement of the cell body attached to the nanostructures, by which
22 the friction forces during cell dividing dynamics may lead to the damage or disruption of cell
23 wall. In contrast, cell divisions of sphere-shaped *Staphylococcus aureus* occur in three
24 dimensions, with the daughter cells remaining nearby leading to grape-like clusters or out-of-
25 plane growth, which resulted in fewer daughter cells in direct contact with the nanocolumnar
26 surface during cell division process, therefore causing less damage to the cell wall by the
27 friction force.^[282] Analogous to black silicon, Hasan *et al.* reported the generation of Ti
28 nanopillars or black Ti (bTi) using a chlorine based reactive ion etching technique. Within
29 4 hours of contact with the bTi surface, 95%±5% of *Escherichia coli*, 98%±2% of
30 *Pseudomonas aeruginosa*, 92%±5% of *Mycobacterium smegmatis* and 22%±8% of
31 *Staphylococcus aureus* cells that had attached were killed. The killing efficiency for the
32 *Staphylococcus aureus* increased to 76%±4% when the bacterial cells were allowed to adhere
33 up to 24 hours.^[283]

1
2
3
4
5
6
7
8
9
10
11
12
13
14
15
16
17
18
19
20
21
22
23
24
25
26
27
28
29
30
31
32
33
34
35
36
37
38
39
40
41
42
43
44
45
46
47
48
49
50
51
52
53
54
55
56
57
58
59
60
61
62
63
64
65

Polymers are also widely used in medical devices such as catheters, feeding tubes, contact lenses, dental prostheses and orthopedic implants. Nanopatterned surfaces can be fabricated using nanoimprinting and colloidal lithography, both are line-of-sight 2D processes. Dickson *et al.* found that nanopillars replicated from imprinting of lithographically produced moulds and cicada wings were bactericidal against *Escherichia coli*. Sharper, more closely packed nanopillars were more effective, possibly because bacteria on these surfaces both contacted more nanopillars and experienced higher stresses at these contact points,^[285] which was in agreement with that found in different insect species.^[263] Replication of moth eye-like nanopillars/cones via nanoimprinting also demonstrated good bactericidal performance in both dry and wet conditions,^[286,287] which could potentially be used for inhibiting nosocomial infections or any sanitation-conscious touching surfaces. Hazzel *et al.* produced similar nanopillar/cone surfaces using colloidal microbeads as masks followed by RIE. It was shown again that surfaces with the most densely packed nanopillar/cone arrays (center-to-center spacing of 200 nm), higher aspect ratios (<3) and sharp tip widths (>20 nm) killed the highest percentage of bacteria (~30 %).^[288]

It is worth noting that the exact mechanisms of bacteria-killing by nanostructures are still not completely clear. One of the most-widely accepted mechanisms is the physical deformation or rupturing of bacterial cell wall/membrane by sharp nanopillars.^[262] However, other mechanisms cannot be ruled out, depending on the nano-feature size and structural process of bacterial cell division. For example, the physical entrapment of bacteria within nanopillars or nanowires may impede the proliferation and growth of bacteria.^[280] The friction forces exerted on the Gram-negative bacterial cell wall during their division process may also result in the damage of bacterial cell wall.^[282] It is therefore important to elucidate the nanotopography-induced antibacterial mechanisms in order to rationally design and fabricate nanostructures for relevant biomedical applications.

6. Cell-instructive (osteogenic and antibacterial) nanotopographies

For many biomedical applications, surfaces with cell-instructive or cell-selective functionalities that are able to control the fate of both mammalian and bacterial cells at the same time are highly desirable. As previously discussed, orthopaedic implants provide a good example of a sector requiring cell-instructive surfaces that could simultaneously promote osseointegration and prevent bacterial infection. This is because the increased demand for orthopaedic prosthesis

1 is fueled by both aseptic loosening (due to poor osseointegration) or infection (due to bacterial
2 infiltration and biofilm formation).^[10,294]

3
4 The use of topographical cues to selectively modulate cells and bacteria has becoming
5 increasingly reported on, mostly on pure Ti metal and its alloys (e.g. Ti6Al4V) because they
6 are most widely used materials for endosseous implants. For example, Peng et al. reported that
7 concave nanotopographies e.g. TiO₂ nanotube arrays with diameters of 30 to 80 nm grown on
8 Ti substrates via anodization exhibited reduced adhesion and lower colonization of bacterial
9 cells (*Staphylococcus epidermidis*) but enhanced, increased, adhesion of osteogenic cells.^[143]
10 Similar cell-selective behavior was observed on nanoporous surfaces for human gingival FBs
11 and oral bacteria (*Streptococcus mutans*, *Fusobacterium nucleatum* and *Porphyromonas*
12 *gingivalis*).^[295] Different cell-selective behavior has also been reported on convex
13 nanotopographies. Densely packed Ti nanocolumns with diameters of 40 to 60 nm fabricated
14 via glancing angle deposition (GLAD) showed strongly reduced bacterial (*Staphylococcus*
15 *aureus*) adhesion and biofilm formation, while osteoblast cells grew well on such surfaces. The
16 selective cell behaviors were attributed to the ‘lotus leaf effect’ caused by the nanocolumnar
17 arrays and the difference in the dimensions of osteoblast and bacterial cells.^[144]

18
19 Since the recent discovery of high aspect ratio bactericidal nanotopographies as reviewed in
20 part 5, research has been carried out on selective cellular responses of both mammalian cells
21 (OBs, MSCs and other cells) and bacteria to such surfaces. The group of Ivanova demonstrated,
22 for example, that while bSi surfaces killed bacteria, the COS-7 eukaryotic cell model could
23 survive and grow.^[296] In fact, the bactericidal nanotopographies, fabricated from bSi with
24 densely packed nanoneedles, promoted the growth and proliferation of fibroblastic cells. Such
25 nanotopography was not only biocompatible but also reduced inflammatory response in a mice
26 model compared with the flat controls.^[296] For orthopaedic application, however, we need to
27 consider bone forming cells. Diu et al. noted that the metabolic activity of OB (MG63) cells
28 cultured on bactericidal hydrothermal TiO₂ nanowire surfaces was only slightly decreased after
29 14 days of cell culture and that while proliferation of OB cells was slowed, especially on long
30 TiO₂ nanowires that formed secondary ‘pocket’ structures, the cells did grow with time. A
31 noticeable change in cell morphology was that some cells became elongated due to ‘pinning’
32 of osteoblast cells on bactericidal TiO₂ nanowire arrays.^[278] Similar results were reported from
33 other groups using different materials or other cell lines.^[279,281,283]

34
35 Most interestingly, these convex high-aspect-ratio, bactericidal nanotopographies seem capable
36 of directing the differentiation of MSCs into OBs, which could have positive implication to the

1
2
3
4
5
6
7
8
9
10
11
12
13
14
15
16
17
18
19
20
21
22
23
24
25
26
27
28
29
30
31
32
33
34
35
36
37
38
39
40
41
42
43
44
45
46
47
48
49
50
51
52
53
54
55
56
57
58
59
60
61
62
63
64
65

real-world applications in orthopaedic or dental implants where both antimicrobial and osseointegrative properties are vital to ensure their long-term success. Tsimbouri et al. investigated osteogenesis of bactericidal TiO₂ nanowires using a mesenchymal bone marrow stromal cell (BMSC)/bone marrow hematopoietic cell (BMHC) co-culture model where both osteogenesis and osteoclastogenesis can occur.^[297]

Similar to the previous results,^[278] BMSCs were well-spread on shorter ‘fine’ or ‘brush’ nanowire surfaces (2 hours (2h) of anodization) with well-organized cytoskeleton but grew slight less well compared with the polished control. Nevertheless, cell proliferation was impaired when growing on longer ‘coarse’ or ‘niche’ nanowire surfaces (>2h) (Figure 10). Cells tended to ‘trap’ inside the pockets formed by the intertwined nanowires. Interestingly, analysis of osteogenic markers osteopontin (OPN) and osteocalcin (OCN) at the transcript and protein level demonstrated an increase in osteogenesis on the 2h nanowire surface compared with the polished control. This indicated that such a surface could be both bactericidal and osteogenic, thus potentially useful in the development of cell-instructive implants. It is notable that the nanowires also prevented osteoclastogenesis and this could have implication in reducing osteolysis.

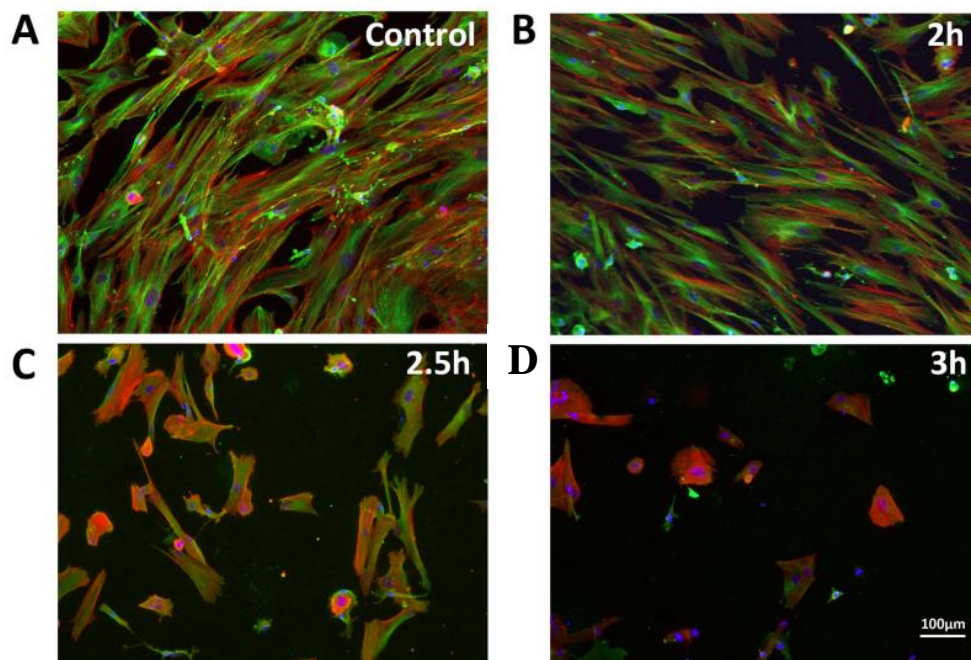


Figure 10. Immunofluorescence micrographs showing cell morphology and spread for BMSCs cultured on different bactericidal TiO₂ nanotopographies. (A) flat control, (B) 2h, (C) 2.5h and (D) 3h surfaces (the length of anodization increasing nanowire size). Notable is that cells on the 2h nanowires spread

well – similar to on planar control. Red: actin, Green: tubulin, Blue: nucleus. **Reproduced under the terms of the Creative Commons Attribution-NonCommercial-NoDerivatives 4.0 International license (CC BY-NC-ND 4.0).**^[278] Copyright 2014, Springer Nature.

7. The synergy of nanotopography and chemical coatings

Nanotopographies with bactericidal potential and capacity to support bone cells populations would be ideal substrates for developing new medical implants, and the recent literature indicates this is possible (see previous Section). However, it is difficult to design cell instructive surfaces with topography alone, i.e. there is typically a reduction in spreading and/or proliferation of bone-related cell types on high aspect ratio bactericidal topographies compared to control Ti surfaces.^[278,283,297] A potential solution to achieve this would be the functionalization of such high aspect-ratio antibacterial topographies with chemical ligands with integrin-binding potential. As discussed in Section 4, it is important for bone forming cells to form “super-mature” focal adhesions (> 5 μm long) in order to stabilize the large OB morphology and thus promote osteogenesis. Thus, a combined topography-chemistry approach could improve cell function on less adherent surfaces.

Fraioli et al. further investigated the use of peptidic ligands combined with bactericidal TiO_2 nanotopographies to improve integrin-specific cell adhesion and hopefully enhance osteogenesis (Figure 11).^[298] It was indeed observed that the functionalization of nanowires by the integrin-binding molecules improved MSCs adhesion significantly (Figure 11C), with increased cell area and formation of larger focal adhesions, which are required for bone formation. Notably, this effect was observed even on the spiky 3h anodization ‘coarse’ nanowire surface, where very poor cell adhesion and proliferation was initially found (Figure 10D).^[278] Further, the study of osteogenic markers confirmed a moderate increase in osteogenesis on the $\alpha\text{v}\beta 3$ -integrin selective peptidomimetic-functionalized nanotopographies. Crucially, the bactericidal properties of the high-aspect-ratio nanotopographies have not been masked by the integrin-binding molecules.

Thus, the functionalization of nanostructured surfaces with chemical coatings should be regarded as a way to improve their cell instructive properties, and offers the possibility to further introduce a wide range of biological activities, which may not be always attainable by topography alone. We showed MSC response can be improved with integrin-binding ligands, while keeping antimicrobial effects; but many other biochemical cues may be introduced, e.g. GFs and osteogenic peptides, mineralization sequences, and even AMPs or other antibacterial

8. Conclusions

1
2 In this review we have shown that both chemical and topographical cues are potent modulators
3 of the functions of eukaryotic and prokaryotic cells. In this regard, modifying the biomaterial
4 surface properties to simultaneously enhance host cell adhesion and function while inhibiting
5 bacterial biofilm formation has been a major focus; we have reported recent strategies that
6 demonstrate this is possible. However, as more efforts are put into developing novel
7 methodologies, the number of challenges increases too.

8
9
10
11
12
13 In the first place, it is becoming evident that the biological evaluation of the osteoconductive
14 and antibacterial potential of any new multifunctional surface will require the use of eukaryotic
15 cell-bacteria co-cultures, as the results obtained with the individual cell types may greatly differ
16 from the more realistic, competitive scenario. In a recent study, we showed that bacteria directly
17 inhibited the capacity of osteoblastic cells to spread and proliferate.^[184] This study indicates
18 that bacteria and cells not only race for the surface, but ‘fight for it’, and makes us postulate
19 that the interactions between these two cell types and the biomaterial surface are better referred
20 to as “the fight for the surface”. However, the mechanisms governing these interactions are not
21 well understood, as the majority of current methods focus on the ‘finish line’,^[14] but do not
22 monitor the dynamic process of competition for the surface. Coupling biomaterials science with
23 biosensing technologies could help to take a step forward to better understand this process.

24
25
26
27
28
29
30
31
32
33
34 Achieving potent osteogenic effects on the biomaterial surface is another challenge. Cell
35 adhesive peptides such as RGD have shown moderate to poor outcomes in animal
36 studies;^[71,72,73] and the delivery of GFs like BMPs, while very effective in inducing bone
37 formation, has raised concerns with regard to unwanted side effects, thus hampering its
38 widespread clinical application.^[90,91] Recent progress on developing multifunctional systems
39 synergizing integrin and GF signaling have shown it is possible to achieve excellent osteogenic
40 responses *in vitro* and bone growth *in vivo*, with only very low doses of GFs.^[86,87,88,89] Such
41 systems may likely represent future strategies for implant-driven osteoinduction. The
42 development of GF-derived, short synthetic peptides and mimetics holds great potential too,
43 and has not been fully explored. The combination of osteogenic peptides with antibacterial
44 agents, like AMPs, has not been investigated either.

45
46
47
48
49
50
51
52
53
54
55 We have also discussed that an increasing concern in the medical device arena is the emergence
56 of bacterial resistance. However, most approaches to fight infections on biomaterials still rely
57 on the use of antibiotics. While is true that newer systems of drug-delivery are being developed,
58 with much better and improved release kinetics, replacement of antibiotics by other
59

1
2
3
4
5
6
7
8
9
10
11
12
13
14
15
antibacterial systems, like the immobilization of AMPs, needs to be further studied. Moreover, some other frequent strategies used in biomaterials research present limitations too. This is the case, for example, of silver, one of the ‘gold standards’ for use in antibacterial surfaces, but that presents toxicity for eukaryotic cells. In response to these limitations, innovations in genomics and the identification of new sources of antibacterial potential are being proposed to fill the classic antibacterial agents gap.^[301 , 302] **Interfering with bacterial quorum sensing communication is another emerging strategy with potential to inhibit biofilm formation on biomaterials.**^[303] Incorporation of such novel antibacterial drugs on biomaterials might well decrease the risk of bacterial resistance.

16
17
18
19
20
21
22
23
24
25
26
27
28
29
30
31
32
33
34
35
36
37
38
39
40
41
42
43
44
45
46
47
48
49
Finally, conferring osteogenic or antibacterial potential to surfaces by pure topographical effects opens up new and promising possibilities in GF- and antibiotic-free medical therapies. Further, achieving both effects by means of topography is a very promising avenue of research and we have shown this is feasible. However, we also acknowledge that this strategy may be limited in terms of bioactivity: the same way bacteria and eukaryotic cells are different in size and morphology, the nanopatterns that maximize one biological effect (e.g. osteogenesis) are in general different from those required to exert the other one (e.g. bacterial kill). This is illustrated by several antibacterial nanopatterns, such as high aspect-ratio surfaces, which effectively kill bacteria, but reduce MSCs functions at the same time. However, we have shown that chemical functionalization of nanotopographies with integrin-binding molecules is a viable way to overcome this hurdle.^[298] Thus, functionalizing nanotopographies with cell adhesive or antibacterial peptides opens new horizons towards highly cell instructive multifunctional biomaterials. The physical bacterial killing mechanism represented by topography is likely to be more evolution resistant than drug-based strategies and the chemical approach can help drive osteogenesis while maintaining bacterial kill. This approach offers an unlimited combination of biological signals for a wide range of applications, and, interestingly, only now is starting to be investigated.

50 **Acknowledgements**

51
52
53
54
55
56
57
58
59
60
61
62
63
64
65
C.M.-M wants to thank the Spanish Government for financial support through a Ramon y Cajal grant (RYC-2015-18566) and Projects No. MAT2015-67183-R and MAT2017-83905-R (MINECO/FEDER), co-funded by the European Union through European Regional Development Funds, the Government of Catalonia (2017 SGR1165) and the European Commission for a Marie Curie Career Integration Grant (REA Grant Agreement No. 321985). M.J.D. thanks the EPSRC for grant EP/K034898/1.

Received: ((will be filled in by the editorial staff))

Revised: ((will be filled in by the editorial staff))

Published online: ((will be filled in by the editorial staff))

References

-
- ¹ M. L. Wolford, K. Palso, A. Bercovitz, Hospitalization for total hip replacement among inpatients aged 45 and over: United States, 2000–2010. NCHS data brief, no 186. Hyattsville, MD: National Center for Health Statistics. 2015.
- ² S. N. Williams, M. L. Wolford, A. Bercovitz, Hospitalization for total knee replacement among inpatients aged 45 and over: United States, 2000–2010. NCHS data brief, no 210. Hyattsville, MD: National Center for Health Statistics. 2015.
- ³ S. Kurtz, K. Ong, E. Lau, F. Mowat, M. Halpern, *J. Bone Joint Surg. Am.* **2007**, *89*, 780.
- ⁴ OECD/EU (2016), Health at a Glance: Europe 2016 – State of Health in the EU Cycle, OECD Publishing, Paris. <http://dx.doi.org/10.1787/9789264265592-en>.
- ⁵ L. Leitner, S. Türk, M. Heidinger, B. Stöckl, F. Posch, W. Maurer-Ertl, A. Leithner, P. Sadoghi, *Sci. Reports* **2018**, *8*, 4707.
- ⁶ J. A. Bishop, A. A. Palanca, M. J. Bellino, D. W. Lowenberg, *J. Am. Acad. Orthop. Surg.* **2012**, *20*, 273.
- ⁷ H. T. Aro, J. J. Alm, N., Moritz, T. J. Makinen, P. Lankinen, *Acta Orthop.* **2012**, *83*, 107.
- ⁸ S. Kurtz, F. Mowat, K. Ong, N. Chan, E. Lau, M. Halpern, *J. Bone Joint Surg. Am.* **2005**, *87*, 1487.
- ⁹ S. B. Goodman, Z. Yao, M. Keeney, F. Yang, *Biomaterials* **2013**, *34*, 3174.
- ¹⁰ J. Raphael, M. Holodniy, S. B. Goodman, S. C. Heilshorn, *Biomaterials* **2016**, *84*, 301.
- ¹¹ R. E. Delanois, J. B. Mistry, C. U. Gwam, N. S. Mohamed, U. S. Choksi, M. A. Mont, *J. Arthroplasty* **2017**, *32*, 2663.
- ¹² R. Adell, U. Lekholm, B. Rockler, P. I Brånemark, *Int. J. Oral Surg.* **1981**, *10*, 387.
- ¹³ C. Mas-Moruno, M. Espanol, E. B. Montufar, G. Mestres, C. Aparicio, F. J. Gil, M. P. Ginebra, in *Biomaterials Surface Science* (Eds: A. Taubert, J. F. Mano, J. C Rodríguez-Cabello), Wiley-VCH, Weinheim, Germany **2013**, pp. 337-374.
- ¹⁴ H. J. Busscher, H. C. van der Mei, G. Subbiahdoss, P. C. Jutte, J. J. M. van denDungen, S. J. Zaat, M. J. Schultz, D. W. Grainger, *Sci. Transl. Med.* **2012**, *4*, 153rv10.
- ¹⁵ S. Veerachamy, T. Yarlagaadda, G. Manivasagam, P. K. Yarlagaadda, Bacterial adherence and biofilm formation on medical implants: a review. *Proc. Inst. Mech. Eng. H J. Eng. Med.* **2014**, *228*, 1083.
- ¹⁶ E. T. J. Rochford, R. G. Richards, T. F. Moriarty, *Clin. Microbiol. Infect.* **2012**, *18*, 1162.
- ¹⁷ P. E. Kolenbrander, R. J. Palmer, S. Periasamy, N. S. Jakubovics, *Nat. Rev. Microbiol.* **2010**, *8*, 471.
- ¹⁸ C. R. Arciola, D. Campoccia, P. Speziale, L. Montanaro, J. W. Costerton, *Biomaterials* **2012**, *33*, 5967.
- ¹⁹ A. H. Holmes, L. S. P. Moore, A. Sundsfjord, M. Steinbakk, S. Regmi, A. Karkey, P. J. Guerin, L. J. V. Piddock, *Lancet* **2016**, *387*, 176.
- ²⁰ W. Costerton, R. Veeh, M. Shirtliff, M. Pasmore, C. Post, G. Ehrlich, *J. Clin. Invest.* **2003**, *112*, 1466.
- ²¹ A. Lee, H. L. Wang, *Implant Dent.* **2010**, *19*, 387.

- 1 22 R. P. Darveau, *Nat. Rev. Microbiol.* **2010**, 8, 481.
- 2 23 K. Vasilev, J. Cook, H. J. Griesser, *Expert Rev. Med. Devices* **2009**, 6, 553.
- 3 24 P. A. Norowski, J. D. Bumgardner, *J. Biomed. Mater. Res. – Part B Appl. Biomater.* **2009**, 88, 530.
- 4 25 M. A. Fernandez-Yague, S. A. Abbah, L. McNamara, D. I. Zeugolis, A. Pandit, M. J. Biggs, *Adv.*
- 5 *Drug Deliver. Rev.* **2015**, 84, 1.
- 6 26 S. Bauer, P. Schmuki, K. von der Mark, J. Park, *Prog. Mater. Sci.* **2013**, 58, 261.
- 7 27 A. Shekaran, A. J. Garcia, *J. Biomed. Mater. Res. A* **2011**, 96, 261.
- 8 28 R. Tejero, E. Anitua, G. Orive, *Prog. Polym. Sci.* **2014**, 39, 1406.
- 9 29 A. Civantos, E. Martínez-Campos, V. Ramos, C. Elvira, A. Gallardo, A. Abarrategi, *ACS Biomater.*
- 10 *Sci. Eng.* **2017**, 3, 1245.
- 11 30 I. Banerjee, R. C. Pangule, R. S. Kane, *Adv. Mater.* **2011**, 23, 690.
- 12 31 K. Glinel, P. Thebault, V. Humblot, C. M. Pradier, T. Jouenne, *Acta Biomater.* **2012**, 8, 1670.
- 13 32 L. Zhang, C. Ning, T. Zhou, X. Liu, K. W. K. Yeung, T. Zhang, Z. Xu, X. Wang, S. Wu, P. K. Chu,
- 14 *ACS Appl. Mater. Interfaces* **2014**, 6, 17323.
- 15 33 E. M. Hetrick, M. H. Schoenfish, *Chem. Soc. Rev.* **2006**, 35, 780.
- 16 34 N. J. Hickok, I. M. Shapiro, *Adv. Drug Deliv. Rev.* **2012**, 64, 1165.
- 17 35 C. Mas-Moruno, in *Peptides and Proteins as Biomaterials for Tissue Regeneration and Repair* (Eds:
- 18 M. A. Barbosa, M. C. L. Martins), Elsevier, Woodhead Publishing, **2018**, pp. 73-100.
- 19 36 K. G. Neoh, X. Hu, D. Zheng, E. T. Kang, *Biomaterials* **2012**, 33, 2813.
- 20 37 S. Spriano, S. Yamaguchi, F. Baino, S. Ferraris, *Acta Biomater.* **2018**, 79, 1.
- 21 38 A. G. Gristina, *Science* **1987**, 237, 1588.
- 22 39 L. Le Guéhennec, A. Soueidan, P. Layrolle, Y. Amouriq, *Dental Mater.* **2007**, 7, 844.
- 23 40 B. D. Bovan, T. W. Hummert, D. D. Dean, Z. Schwartz, *Biomaterials* **1996**, 17, 137.
- 24 41 J. Y. Martin, Z. Schwartz, T. W. Hummert, D. M. Schraub, J. Simpson, J. Jr. Lankford, D. D. Dean,
- 25 D. L. Cochran, B. D. Boyan, *J. Biomed. Mater. Res.* **1995**, 29, 389.
- 26 42 M. Pegueroles, C. Aparicio, M. Bosio, E. Engel, F. J. Gil, J. A. Planell, G. Altankov, *Acta Biomater.*
- 27 **2010**, 6, 291.
- 28 43 C. M. Bollen, W. Papaioanno, J. Van Eldere, E. Schepers, M. Quirynen, D. van Steenberghe, *Clin.*
- 29 *Oral Implants Res.* **1996**, 7, 201.
- 30 44 D. D. Deligianni, N. Katsala, S. Ladas, D. Sotiropoulou, J. Amedee, Y. F. Missirlis, *Biomaterials*
- 31 **2001**, 22, 1241.
- 32 45 K. de Groot, R. Geesink, C. P. Klein, P. Serekian, *J. Biomed. Mater. Res.* **1987**, 21, 1375.
- 33 46 F. Barrere, C. M. van der Valk, G. Meijer, R. A. Dalmeijer, K. de Groot, P. Layrolle, *J. Biomed. Mater.*
- 34 *Res.* **2003**, 67, 655.
- 35 47 R. G. T. Geesink, K. de Groot, C. P. A. T. Klein, *Clin. Orthop.* **1987**, 225, 147.
- 36 48 M. Shrikhanzadeh, *J. Mater. Sci. Lett.* **1991**, 10, 1415.
- 37 49 J. E. Hulshoff, T. Hayakawa, K. van Dijk, A. F. Leijdekkers-Govers, J. P. van der Waerden, J. A.
- 38 Jansen, *J. Biomed. Mater. Res.* **1997**, 36, 75.
- 39 50 J. Lee, L. Rouhfar, O. Beirne, *J. Oral Maxillofac. Surg.* **2000**, 58, 1372.
- 40 51 T. Kokubo, F. Miyaji, H. M. Kim, *J. Amer. Ceram. Soc.* **1996**, 79, 1127.
- 41 52 H. B. Wen, J. R. De Wijn, Q. Liu, K. De Groot, F. Z. Cui, *J. Mater. Sci. Mater. Med.* **1997**, 8, 765.
- 42 53 P. Li, K. De Groot *J. Biomed. Mater. Res.* **1993**, 27, 1445.
- 43 44
- 44
- 45
- 46
- 47
- 48
- 49
- 50
- 51
- 52
- 53
- 54
- 55
- 56
- 57
- 58
- 59
- 60
- 61
- 62
- 63
- 64
- 65

- 1 54 A. A. Campbell, G. Fryxell, J. Linehan, *G. J. Biomed. Mater. Res.* **1996**, 32, 111.
2
3 55 C. Ohtsuki, H. Iida, S. Hayakawa, A. Osaka, *J. Biomed. Mater. Res.* **1997**, 35, 39.
4
5 56 P. Li, P. Ducheyne, *J. Biomed. Mater. Res.* **1998**, 41, 341.
6
7 57 X. Wang, W. Yan, S. Hayakawa, K. Tsuru, A. Osaka, *Biomaterials* **2003**, 24, 4631.
8
9 58 S. Nishiguchi, H. Kato, H. Fujita, M. Oka, H. M. Kim, T. Kokubo, T. Nakamura, *Biomaterials* **2001**,
10 22, 2525.
11 59 T. Miyaza, H. M. Kim, T. Kokubo, C. Ohtsuki, H. Kato, T. Nakamura, *Biomaterials* **2002**, 23, 827.
12 60 M. Uchida, H. M. Kim, F. Miyaji, T. Kokubo, T. Nakamura, *Biomaterials* **2002**, 23, 313.
13 61 T. Kokubo, H. M. Kim, M. Kawashita, T. Nakamura, *J. Mater. Sci. Mater. Med.* **2004**, 15, 99.
14 62 G. Bhardwaj, H. Yazici, T. J. Webster, *Nanoscale* **2015**, 7, 8416.
15 63 M. P. Ginebra, C. Canal, M. Espanol, D. Pastorino, E. B. Montufar, *Adv. Drug Deliv. Rev.* **2012**, 64,
16 1090.
17 64 A. E. Rodda, L. Meagher, D. R. Nisbet, J. S. Forsythe, *Prog. Polym. Sci.* **2014**, 39, 1312.
18 65 K. von der Mark, J. Park, *Prog. Mater. Sci.* **2013**, 58, 327.
19 66 M. D. Pierschbacher, E. Ruoslahti, *Nature* **1984**, 309, 30.
20 67 M. D. Pierschbacher, E. Ruoslahti, *Cell* **1986**, 44, 517.
21 68 R. O. Hynes, *Cell* **2002**, 110, 673.
22 69 U. Hersel, C. Dahmen, H. Kessler, *Biomaterials* **2003**, 24, 4385.
23 70 C. Mas-Moruno, R. Fraioli, F. Rechenmacher, S. Neubauer, T. G. Kapp, H. Kessler, *Angew. Chem.*
24 *Int. Ed.* **2016**, 55, 7048.
25 71 S. L. Bellis, *Biomaterials* **2011**, 32, 4205.
26 72 T. H. Barker, *Biomaterials* **2011**, 32, 4211.
27 73 J. H. Collier, T. Segura, *Biomaterials* **2011**, 32, 4198.
28 74 T. A. Petrie, J. R. Capadona, C. D. Reyes, A. J. Garcia, *Biomaterials* **2006**, 27, 5459.
29 75 T. A. Petrie, J. E. Raynor, C. D. Reyes, K. L. Burns, D. M. Collard, A. J. García, *Biomaterials* **2008**,
30 29, 2849.
31 76 R. Agarwal, C. González-García, B. Torstrick, R. E. Guldberg, M. Salmerón-Sánchez, A. J. García,
32 *Biomaterials* **2015**, 63, 137.
33 77 C. Herranz-Diez, C. Mas-Moruno, S. Neubauer, H. Kessler, F. J. Gil, M. Pegueroles, J. M. Manero,
34 J. Guillem-Martí, *ACS Appl. Mater. Interfaces* **2016**, 8, 2517.
35 78 C. Mas-Moruno, R. Fraioli, F. Albericio, J. M. Manero, F. J. Gil, *ACS Appl. Mater. Interfaces* **2014**,
36 6, 6525.
37 79 R. Fraioli, K. Dashnyam, J. H. Kim, R. A. Perez, H. W. Kim, J. Gil, M. P. Ginebra, J. M. Manero, C.
38 Mas-Moruno, *Acta Biomater.* **2016**, 43, 269.
39 80 M. Pagel, R. Hassert, T. John, K. Braun, M. Wießler, B. Abel, A. G. Beck-Sicking, *Angew. Chemie*
40 *Int. Ed.* **2016**, 55, 4826.
41 81 R. Fraioli, F. Rechenmacher, S. Neubauer, J. M. Manero, J. Gil, H. Kessler, C. Mas-Moruno, *Colloid.*
42 *Surf. B.* **2015**, 128, 191.
43 82 B. Bragdon, O. Moseychuk, S. Saldanha, D. King, J. Julian, A. Nohe, *Cell. Signal.* **2011**, 23, 609.
44 83 Q. Wei, T. L. M. Pohl, A. Seckinger, J. P. Spatz, E. A. Cavalcanti-Adam, *Beilstein J. Org. Chem.*
45 **2015**, 11, 773.
46 84 M. Salmerón-Sánchez, M. J. Dalby, *Chem. Commun.* **2016**, 52, 13327.

- 1 85 M. M. Martino, P. S. Briquez, K. Maruyama, J. A. Hubbell, *Adv. Drug Deliv. Rev.* **2015**, *94*, 41.
2
3 86 M. Kisiel, M. M. Martino, M. Ventura, J. A. Hubbell, J. Hilborn, D. A. Ossipov, *Biomaterials* **2013**,
4 *34*, 704.
5 87 M. M. Martino, F. Tortelli, M. Mochizuki, S. Traub, D. Ben-David, G. A. Kuhn, R. Muller, E. Livne,
6 S. A. Eming, J. A. Hubbell, *Sci. Transl. Med.* **2011**, *3*, 100ra89.
7
8 88 A. Shekaran, J. R. García, A. Y. Clark, T. E. Kavanaugh, A. S. Lin, R. E. Guldborg, A. J.
9 García, *Biomaterials* **2014**, *35*, 5453.
10
11 89 V. Llopis-Hernández, M. Cantini, C. González-García, Z. A. Cheng, J. Yang, P. M. Tsimbouri, A. J.
12 García, M. J. Dalby, M. Salmerón-Sánchez, *Sci Adv.* **2016**, *2*, e1600188.
13
14 90 E. J. Carragee, E. L. Hurwitz, B. K. A. Weiner, *Spine J.* **2011**, *11*, 471.
15
16 91 E. J. Carragee, G. Chu, R. Rohatgi, E. L. Hurwitz, B. K. Weiner, S. T. Yoon, G. Comer, B. Kopjar, *J.*
17 *Bone Joint Surg. Am.* **2013**, *95*, 1537.
18
19 92 T. Fowler, E. R. Wann, D. Joh, S. Johansson, T. J. Foster, M. Höök, *Eur. J. Cell Biol.* **2000**, *79*, 672.
20
21 93 U. Schwarz-Linek, J. M. Werner, A. R. Pickford, S. Gurusiddappa, J. H. Kim, E. S. Pilka, J. A. Briggs,
22 T. S. Gough, M. Höök, I. D. Campbell, J. R. Potts, *Nature* **2003**, *423*, 177.
23
24 94 J. M. Patti, J. O. Boles, M. Hook, *Biochemistry* **1993**, *32*, 11428.
25
26 95 C. Aparicio, F. J. Gil, C. Fonseca, M. Barbosa, J. A. Planell, *Biomaterials* **2003**, *24*, 263.
27
28 96 C. Aparicio, J. M. Manero, F. Conde, M. Pegueroles, J. A. Planell, M. Vallet-Regi, F. J. Gil, *J. Biomed.*
29 *Mater. Res. A* **2007**, *82*, 521.
30
31 97 C. Aparicio, F. J. Gil, J. A. Planell, E. Engel, *J. Mater. Sci. Mater. Med.* **2002**, *13*, 1105.
32
33 98 C. Aparicio, A. Padros, F. J. Gil, *J. Mech. Behav. Biomed. Mater.* **2011**, *4*, 1672.
34
35 99 C. Mas-Moruno, P. M. Dorfner, F. Manzenrieder, S. Neubauer, U. Reuning, R. Burgkart, H. Kessler,
36 *J. Biomed. Mater. Res. Part A* **2013**, *101*, 87.
37
38 100 K. G. Neoh, E. T. Kang, *ACS Appl. Mater. Interfaces* **2011**, *3*, 2808.
39
40 101 O'Neill, J. Tackling drug-resistant infections globally: final report and recommendations. The review
41 on antimicrobial resistance. May 2016. Wellcome Trust. London, UK.
42
43 102 S. Buffet-Bataillon, P. Tattevin, M. Bonnaure-Mallet, A. Jolivet-Gougeon, *Int. J. Antimicrob. Agents*
44 **2012**, *39*, 381.
45
46 103 K. Hiramatsu, Y. Katayama, M. Matsuo, T. Sasaki, Y. Morimoto, A. Sekiguchi, T. Baba, *J. Infect.*
47 *Chemother.* **2014**, *20*, 593.
48
49 104 O. Bondarenko, K. Juganson, A. Ivask, K. Kasemets, M. Mortimer, A. Kahru, *Arch. Toxicol.* **2013**,
50 *87*, 1181.
51
52 105 N. Duewelhenke, O. Krut, P. Eysel, *Antimicrob. Agents Chemother.* **2007**, *51*, 54.
53
54 106 L. G. Harris, S. Tosatti, M. Wieland, M. Textor, R. G. Richards, *Biomaterials* **2004**, *25*, 4135.
55
56 107 R. R. Maddikeri, S. Tosatti, M. Schuler, S. Chessari, M. Textor, R. G. Richards, L. G. Harris, *J.*
57 *Biomed. Mater. Res. Part A* **2008**, *84*, 425.
58
59 108 G. Subbiahdoss, B. Pidhatika, G. Coullerez, M. Charnley, R. Kuijjer, *Eur. Cells Mater.* **2010**, *19*, 205.
60
61 109 J. Buxadera-Palomero, C. Calvo, S. Torrent-Camarero, F. J. Gil, C. Mas-Moruno, C. Canal, D.
62 Rodríguez, *Colloid Surf. B Biointerfaces* **2017**, *152*, 367.
63
64 110 Z. Shi, K. G. Neoh, E. T. Kang, C. Poh, W. Wang, *Tissue Eng. Part A* **2009**, *15*, 417.
65
66 111 F. Zhang, Z. Zhang, X. Zhu, E. T. Kang, K. G. Neoh, *Biomaterials* **2008**, *29*, 4751.
67
68 112 X. Hu, K. G. Neoh, Z. Shi, E. T. Kang, C. Poh, W. Wang, *Biomaterials* **2010**, *31*, 8854.

- 1 ¹¹³ Q. Yu, Z. Wu, H. Chen, *Acta Biomater.* **2015**, *16*, 1.
- 2 ¹¹⁴ S. Yan, L. Song, S. Luan, Z. Xin, S. Du, H. Shi, S. Yuan, Y. Yang, J. Yin, *Colloids Surf. B*
- 3 *Biointerfaces* **2017**, *150*, 250.
- 4 ¹¹⁵ J.-B. Paris, D. Seyer, T. Jouenne, P. Thébault, *Colloids Surf. B Biointerfaces* **2017**, *156*, 186.
- 5 ¹¹⁶ Q. Gao, M. Yu, Y. Su, M. Xie, X. Zhao, P. Li, P.X. Ma, *Acta Biomater.* **2017**, *51*, 112.
- 6 ¹¹⁷ C. Yang, X. Ding, R.J. Ono, H. Lee, L.Y. Hsu, Y.W. Tong, J. Hedrick, Y.Y. Yang, *Adv. Mater.* **2014**,
- 7 *26*, 7346.
- 8 ¹¹⁸ Y. Su, Z. Zhi, Q. Gao, M. Xie, M. Yu, B. Lei, P. Li, P.X. Ma, *Adv. Healthc. Mater.* **2017**, *6*, 1.
- 9 ¹¹⁹ Z. Zhi, Y. Su, Y. Xi, L. Tian, M. Xu, Q. Wang, S. Padidan, P. Li, W. Huang, *ACS Appl. Mater.*
- 10 *Interfaces* **2017**, *9*, 10383.
- 11 ¹²⁰ M. Dash, F. Chiellini, R.M. Ottenbrite, E. Chiellini, *Prog. Polym. Sci.* **2011**, *36*, 981.
- 12 ¹²¹ P. Chua, K. Neoh, E. Kang, W. Wang, *Biomaterials* **2008**, *29*, 1412.
- 13 ¹²² Z. Shi, K. G. Neoh, E. T. Kang, C. Poh, W. Wang, *J. Biomed. Mater. Res. Part A.* **2008**, *86*, 865.
- 14 ¹²³ Z. Shi, K. G. Neoh, E. T. Kang, C. K. Poh, W. Wang, *Biomacromolecules* **2009**, *10*, 1603.
- 15 ¹²⁴ L. Han, H. Lin, X. Lu, W. Zhi, K.- f. Wang, F.- z. Meng, O. Jiang, *Mater. Sci. Eng. C* **2014**, *40*, 1.
- 16 ¹²⁵ D. Zheng, K. G. Neoh, E. T. Kang, *Appl. Surf. Sci.* **2016**, *360*, 86.
- 17 ¹²⁶ M. A. Bonifacio, S. Cometa, M. Dicarlo, F. Baruzzi, S. de Candia, A. Gloria, M. M. Giangregorio,
- 18 M. Mattioli-Belmonte, E. De Giglio, *Carbohydr. Polym.* **2017**, *166*, 348.
- 19 ¹²⁷ A. Jain, L. S. Duvvuri, S. Farah, N. Beyth, A. J. Domb, W. Khan, *Adv. Healthcare Mater.* **2014**, *3*,
- 20 **1969**.
- 21 ¹²⁸ R. Ye, H. Xu, C. Wan, S. Peng, L. Wang, H. Xu, Z. P. Aguilar, Y. Xiong, Z. Zeng, H. Wei, *Biochem.*
- 22 *Biophys. Res. Commun.* **2013**, *439*, 148.
- 23 ¹²⁹ R. Wang, D.-l. Xu, L. Liang, T.-t. Xu, W. Liu, P.-k. Ouyang, B. Chi, H. Xu, *RSC Adv.* **2016**, *6*, 8620.
- 24 ¹³⁰ R. Wang, J. Li, W. Chen, T. Xu, S. Yun, Z. Xu, Z. Xu, T. Sato, B. Chi, H. Xu, *Adv. Funct. Mater.*
- 25 **2017**, *27*, 1604894.
- 26 ¹³¹ Y. Cheng, H. Yang, Y. Yang, J. Huang, K. Wu, Z. Chen, X. Wang, C. Lin, Y. Lai, *J. Mater. Chem.*
- 27 *B*, **2018**, *6*, 1862.
- 28 ¹³² K. Das, S. Bose, A. Bandyopadhyay, B. Karandikar, B. L. Gibbins, *J. Biomed. Mater. Res. Part B*
- 29 **2008**, *87*, 455.
- 30 ¹³³ L. Zhao, H. Wang, K. Huo, L. Cui, W. Zhang, H. Ni, Y. Zhang, Z. Wu, P. K. Chu, *Biomaterials* **2011**,
- 31 *32*, 5706.
- 32 ¹³⁴ A. Gao, R. Hang, X. Huang, L. Zhao, X. Zhang, L. Wang, B. Tang, S. Mad, P. K. Chu, *Biomaterials*
- 33 **2014**, *35*, 4223.
- 34 ¹³⁵ K. Huo, X. Zhang, H. Wang, L. Zhao, X. Liu, P.K. Chu, *Biomaterials* **2013**, *34*, 3467.
- 35 ¹³⁶ Y. Li, W. Xiong, C. Zhang, B. Gao, H. Guan, H. Cheng, J. Fu, F. Li, *J. Biomed. Mater. Res. Part A*
- 36 **2014**, *102*, 3939.
- 37 ¹³⁷ R. Hang, A. Gao, X. Huang, X. Wang, X. Zhang, L. Qin, B. Tang, *J. Biomed. Mater. Res. A* **2014**,
- 38 *102*, 1850.
- 39 ¹³⁸ K. C. Popat, M. Eltgroth, T. J. Latempa, C. A. Grimes, T. A. Desai, *Biomaterials* **2007**, *28*, 4880.
- 40 ¹³⁹ T. Kumeria, H. Mon, M. S. Aw, K., Gulati, A. Santos, H. J. Griesser, D. Losic, *Colloid Surf. B*
- 41 *Biointerfaces* **2014**, *130*, 255.
- 42 ¹⁴⁰ S. Mei, H. Wang, W. Wang, L. Tong, H. Pan, C. Ruan, Q. Ma, M. Liu, H. Yang, L. Zhang, Y. Cheng,
- 43
- 44
- 45
- 46
- 47
- 48
- 49
- 50
- 51
- 52
- 53
- 54
- 55
- 56
- 57
- 58
- 59
- 60
- 61
- 62
- 63
- 64
- 65

- 1 Y. Zhang, L. Zhao, P. K. Chu, *Biomaterials* **2014**, *35*, 4255.
- 2
3 ¹⁴¹ A. Roguska, A. Belcarz, M. Pisarek, G. Ginalska, M. Lewandowska, *Mater. Sci. Eng. C* **2015**, *51*,
4 158.
- 5 ¹⁴² P. J. Finley, R. Norton, C. Austin, A. Mitchell, S. Zank, P. Durham, *Antimicrob. Agents Chemother.*
6 **2015**, *59*, 4734.
- 7
8 ¹⁴³ Z. Peng, J. Ni, K. Zheng, Y. Shen, X. Wang, G. He, S. Jin, T. Tang, *Int. J. Nanomed.* **2013**, *8*, 3093.
- 9
10 ¹⁴⁴ I. Izquierdo-Barba, J. M. Garcia-Martin, R. Alvarez, A. Palmero, J. Esteban, C. Perez-Jorge, D. Arcos,
11 M. Vallet-Regí, *Acta Biomater.* **2015**, *15*, 20.
- 12
13 ¹⁴⁵ W. Chen, Y. Liu, H. S. Courtney, M. Bettenga, C. M. Agrawal, J. D. Bumgardner, J. L. Ong,
14 *Biomaterials* **2006**, *27*, 5512.
- 15
16 ¹⁴⁶ W. Chen, S. Oh, A. P. Ong, N. Oh, Y. Liu, H. S. Courtney, M. Appleford, J. L. Ong, *J. Biomed.*
17 *Mater. Res. A* **2007**, *82*, 899.
- 18
19 ¹⁴⁷ A. Besinis, S. D. Hadi, H. R. Le, C. Tredwin, R. D. Handy, *Nanotoxicology* **2017**, *11*, 327.
- 20
21 ¹⁴⁸ M. A. Surmeneva, A. A. Sharonova, S. Chernousova, O. Prymak, K. Loza, M. S. Tkachev, I. A.
22 Shulepov, M. Epple, R. A. Surmenev, *Colloids Surf. B Biointerfaces* **2017**, 156, 104.
- 23 ¹⁴⁹ C.-M. Xie, X. Lu, K.-F. Wang, F.-Z. Meng, O. Jiang, H.-P. Zhang, W. Zhi, L.-M. Fang, *ACS Appl.*
24 *Mater. Interfaces* **2014**, *6*, 8580.
- 25
26 ¹⁵⁰ G. A. Fielding, M. Roy, A. Bandyopadhyay, S. Bose, *Acta Biomater.* **2012**, *8*, 3144.
- 27
28 ¹⁵¹ Z. Geng, Z. Cui, Z. Li, S. Zhu, Y. Liang, Y. Liu, X. Li, X. He, X. Yu, R. Wang, X. Yang, *Mater. Sci.*
29 *Eng. C* **2016**, *58*, 467.
- 30
31 ¹⁵² Z. Geng, R. Wang, X. Zhuo, Z. Li, Y. Huang, L. Ma, Z. Cui, S. Zhu, Y. Liang, Y. Liu, H. Bao, X.
32 Li, Q. Huo, Z. Liu, X. Yang, *Mater. Sci. Eng. C* **2017**, *71*, 852.
- 33
34 ¹⁵³ M. Kazemzadeh-Narbat, J. Kindrachuk, K. Duan, H. Jenssen, R. E. Hancock, R. Wang, *Biomaterials*
35 **2010**, *31*, 9519.
- 36
37 ¹⁵⁴ M. Kazemzadeh-Narbat, S. Noordin, B. A. Masri, D. S. Garbuz, C. P. Duncan, R. E. W. Hancock, R.
38 Wang, *J. Biomed. Mater. Res. B Appl. Biomater.* **2012**, *100*, 1344.
- 39
40 ¹⁵⁵ V. Alt, A. Bitschnau, J. Osterling, A. Sewing, C. Meyer, R. Kraus, S. A. Meissner, S. Wenisch, E.
41 Domann, R. Schnettler, *Biomaterials* **2006**, *27*, 4627.
- 42
43 ¹⁵⁶ S. Radin, J. T. Campbell, P. Ducheyne, J. M. Cuckler, *Biomaterials* **1997**, *18*, 777.
- 44
45 ¹⁵⁷ H. Gautier, G. Daculsi, C. Merle, *Biomaterials* **2001**, *22*, 2481.
- 46
47 ¹⁵⁸ C. J. Pan, Y. X. Dong, Y. Y. Zhang, Y. D. Nie, C. H. Zhao, Y. L. Wang, *J. Orthop. Sci.* **2011**, *16*,
48 105.
- 49
50 ¹⁵⁹ V. Uskokovic, C. Hoover, M. Vukomanovic, D.P. Uskokovic, T.A. Desai, *Mater. Sci. Eng. C Mater.*
51 *Biol. Appl.* **2013**, *33*, 3362.
- 52
53 ¹⁶⁰ M. Kazemzadeh-Narbat, B. F. Lai, C. Ding, J. N. Kizhakkedathu, R. E. Hancock, R. Wang,
54 *Biomaterials* **2013**, *34*, 5969.
- 55
56 ¹⁶¹ C. Labay, J. M. Canal, M. Modic, U. Cvelbar, M. Quiles, M. Armengol, M. A. Arbos, F. J. Gil, C.
57 Canal, *Biomaterials* **2015**, *71*, 132.
- 58
59 ¹⁶² C. Canal, M. Modic, U. Cvelbar, M. P. Ginebra, *Biomater. Sci.* **2016**, *4*, 1454.
- 60
61 ¹⁶³ U. K. Marelli, F. Rechenmacher, T. R. Sobahi, C. Mas-Moruno, H. Kessler, *Front. Oncol.* **2013**, *3*,
62 222.
- 63
64 ¹⁶⁴ P. Rocas, M. Hoyos-Nogues, J. Rocas, J. M. Manero, J. Gil, F. Albericio, C. Mas-Moruno, *Adv.*
65 *Healthcare Mater.* **2015**, *4*, 1956.

- 165 E. M. Hetrick, M. H. Schoenfisch, *Chem. Soc. Rev.* **2006**, 35, 780.
- 166 M. Zilberman, J. J. Elsner, *J. Controlled Release* **2008**, 130, 202.
- 167 Z. Wang, K. Wang, X. Lu, C. Li, L. Han, C. Xie, Y. Liu, S. Qu, G. Zhen, *Adv. Healthcare Mater.* **2015**, 4, 927.
- 168 L. Han, Z.-m. Wang, X. Lu, L. Dong, C.-m. Xie, K.-f. Wang, X.-l. Chen, Y.-h. Ding, L.-t. Weng, *Colloids Surf. B Biointerfaces* **2015**, 126, 452.
- 169 D. S. W. Benoit, K. S. Anseth, *Biomaterials* **2005**, 26, 5209.
- 170 M. Schuler, D. W. Hamilton, T. P. Kunzler, C. M. Sprecher, M. de Wild, D. M. Brunette, M. Textor, S. G. P. Tosatti, *J. Biomed. Mater. Res. Part B* **2009**, 91, 517.
- 171 B. F. Bell, M. Schuler, S. Tosatti, M. Textor, Z. Schwartz, B. D. Boyan, *Clin. Oral Implants Res.* **2011**, 22, 865.
- 172 N. M. Moore, N. J. Lin, N. D. Gallant, M. L. Becker, *Acta Biomater.* **2011**, 7, 2091.
- 173 W. N. Yin, F. Y. Cao, K. Han, X. Zeng, R. X. Zhuo, X. Z. Zhang, *J. Mater. Chem. B* **2014**, 2, 8434.
- 174 M. Pagel, A. G. Beck-Sickinger, *Biol. Chem.* **2017**, 398, 3.
- 175 J. M. Ageitos, A. Sánchez-Pérez, P. Calo-Mata, T. G. Villa, *Biochem. Pharmacol.* **2017**, 133, 117.
- 176 C. De La Fuente-Núñez, M. H. Cardoso, E. De Souza Cândido, O. L. Franco, R. E. W. Hancock, *Biochim. Biophys. Acta – Biomembr.* **2016**, 1858, 1061.
- 177 N. Stempel, J. Strehmel, J. Overhage, *Curr. Pharm. Des.* **2015**, 21, 67.
- 178 M. Riool, A. de Breij, J. W. Drijfhout, P. H. Nibbering, S. A. J. Zaat, *Front. Chem.* **2017**, 5, 63.
- 179 W. Lin, C. Junjian, C. Chengzhi, S. Lin, L. Sa, R. Li, W. Yingjun, *J. Mater. Chem. B* **2015**, 3, 30.
- 180 M. Godoy-Gallardo, C. Mas-Moruno, M. C. Fernández-Calderón, C. Pérez-Giraldo, J. M. Manero, F. Albericio, F. J. Gil, D. Rodriguez, *Acta Biomater.* **2014**, 10, 3522.
- 181 M. Godoy-Gallardo, C. Mas-Moruno, K. Yu, J. M. Manero, F. J. Gil, J. N. Kizhakkedathu, D. Rodriguez, *Biomacromolecules* **2015**, 16, 483.
- 182 M. Hoyos-Nogués, F. Velasco, M.- P. Ginebra, J. M. Manero, F. J. Gil, C. Mas-Moruno, *ACS Appl. Mater. Interfaces* **2017**, 9, 21618.
- 183 H. H. Tuson, D. B. Weibel, *Soft Matter* **2013**, 9, 4368.
- 184 M. Hoyos-Nogués, J. Buxadera-Palomero, M. P. Ginebra, J. M. Manero, F. J. Gil, C. Mas-Moruno, *Colloids Surf. B Biointerfaces* **2018**, 169, 30.
- 185 A. K. Muszanska, E. T. J. Rochford, A. Gruszka, A. A. Bastian, H. J. Busscher, W. Norde, H. C. Van Der Mei, A. Herrmann, *Biomacromolecules* **2014**, 15, 2019.
- 186 E. Yüksel, A. Karakeçili, T. T. Demirtas, M. Gümüşderelioglu, *Int. J. Biol. Macromol.* **2016**, 86, 162.
- 187 E. Jabbari, *Curr. Pharm. Des.* **2013**, 19, 3391.
- 188 F. R. Maia, S. J. Bidarra, P. L. Granja, C. C. Barrias, *Acta Biomater.* **2013**, 9, 8773.
- 189 J. K. Bronk, B. H. Russell, J. J. Rivera, R. Pasqualini, W. Arap, M. Hook, E. Magda Barbu, *Acta Biomater.* **2014**, 10, 3354.
- 190 M. Godoy-Gallardo, J. Guillem-Martí, P. Sevilla, J. M. Manero, F. J. Gil, D. Rodriguez, *Mater. Sci. Eng. C* **2016**, 59, 524.
- 191 S. Yuran, A. Dolid, M. Reches, *ACS Biomater. Sci. Eng.*, DOI: 10.1021/acsbiomaterials.8b00885
- 192 A. Ponche, M. Bigerelle, K. Anselme, *Proc. Inst. Mech. Eng. H* **2010**, 224, 1471.
- 193 R. A. Gittens, R. Olivares-Navarrete, Z. Schwartz, B. D. Boyan, *Acta Biomater.* **2014**, 10, 3363.
- 194 R. Harrison, *Science* **1911**, 34, 279.

- 195 P. Weiss, B. Garber, *Proc. Natl. Acad. Sci. USA* **1952**, 38, 264.
- 196 A. S. Curtis, M. Varde, *J. Nat. Cancer Res. Inst.* **1964**, 33, 15.
- 197 A. S. Curtis, *Eur. Cells Mater.* **2004**, 8, 27.
- 198 C. D. W. Wilkinson, *Eur. Cells Mater.* **2004**, 8, 21.
- 199 A. S. Curtis, C. D. Wilkinson, *J. Biomater. Sci. Polym. Ed.* **1998**, 9, 1313.
- 200 A. Curtis, C. Wilkinson, *Biomaterials* **1997**, 18, 1573.
- 201 S. Britland, H. Morgan, B. Wojciak-Stodart, M. Riehle, A. Curtis, C. Wilkinson, *Exp. Cell Res.* **1996**, 228, 313.
- 202 B. Wojciak-Stothard, A. S. Curtis, W. Monaghan, M. McGrath, I. Sommer, C. D. Wilkinson, *Cell Motility Cytoskeleton* **1995**, 31, 147.
- 203 B. Wojciak-Stothard, Z. Madeja, W. Korohoda, A. Curtis, C. Wilkinson, *Cell Biol. Int.* **1995**, 19, 485.
- 204 P. Clark, P. Connolly, A. S. Curtis, J. A. Dow, C. D. Wilkinson, *Development* **1990**, 108, 635.
- 205 P. Clark, P. Connolly, A. S. Curtis, J. A. Dow, C. D. Wilkinson, *Development* **1987**, 99, 439.
- 206 P. Clark, P. Connolly, A. S. Curtis, J. A. Dow, C. D. Wilkinson, *J. Cell. Sci.* **1991**, 99 (Pt1), 73.
- 207 C. Vieu, F. Carcenac, A. Pépin, Y. Chen, M. Mejias, A. Lebib, L. Manin-Ferlazzo, L. Couraud, H. Launois, *Appl. Surf. Sci.* **2000**, 164, 111.
- 208 F. A. Denis, P. Hanarp, D. S. Sutherland, J. Gold, C. Mustin, P. G. Rouxhet, Y. F. Dufrêne, *Langmuir* **2002**, 18, 19.
- 209 P. Hanarp, D. Sutherland, J. Gold, B. Kasemo, *Nanostruct. Mater* **1999**, 12, 429.
- 210 S. Affrossman, M. Stamm, *Colloid Polym. Sci.* **2000**, 278, 888.
- 211 S. Affrossman, R. Jerome, S. A. O'Neill, T. Schmitt, M. Stamm, *Colloid Polym. Sci.* **2000**, 278, 993.
- 212 S. Krishnamoorthy, C. Hibert, M. Liley, A. Meister, M. Dalby, R. Oreffo, J. Brugger, R. Pugin, H. Heinzelmann, C. Hinderling, In *International Conference on Nanoscience and Technology ICN&T; 2006*.
- 213 S. Krishnamoorthy, R. Pugin, M. Liley, M. J. Dalby, R. Oreffo, H. Heinzelmann, J. Brugger, C. Hinderling, In *Biosurf. VI-Tissue-Surface Interaction; 2005*.
- 214 M. Dalby, M. Riehle, H. Johnstone, S. Affrossman, A. Curtis, *Biomaterials* **2002**, 23, 2945.
- 215 E. K. Yim, R. M. Reano, S. W. Pang, A. F. Yee, C. S. Chen, K. W. Leong, *Biomaterials* **2005**, 26, 5405.
- 216 A. S. G. Curtis, N. Gadegaard, M. J. Dalby, M. O., Riehle, C. D. W. Wilkinson, G. Aitchison, *NanoBioscience, IEEE Transactions* **2004**, 3, 61.
- 217 N. Gadegaard, S. Thoms, D. S. Macintyre, K. Mcghee, J. Gallagher, B. Casey, C. D. W. Wilkinson, *Microelectronic Engineering* **2003**, 67-68, 162.
- 218 F. A. Denis, P. Hanarp, D. S. Sutherland, Y. F. Dufrene, *Nano Lett.* **2002**, 2, 1419.
- 219 E. M. Hur, K. T. Kim, *Cell Signal* **2002**, 14, 397.
- 220 J. Huang, S. V. Grater, F. Corbellini, S. Rinck, E. Bock, R. Kemkemer, H. Kessler, J. Ding, J. P. Spatz, *Nano Lett.* **2009**, 9, 1111.
- 221 R. J. McMurray, N. Gadegaard, P. M. Tsimbouri, K. V. Burgess, L. E. McNamara, R. Tare, K. Murawski, E. Kingham, R. O. Oreffo, M. J. Dalby, *Nat. Mater.* **2011**, 10, 637.
- 222 M. J. Dalby, N. Gadegaard, R. Tare, A. Andar, M. O. Riehle, P. Herzyk, C. D. Wilkinson, R. O. Oreffo, *Nat. Mater.* **2007**, 6, 997.
- 223 S. Krishnamoorthy, R. Pugin, J. Brugger, H. Heinzelmann, A. C. Hoogerwerf, C. Hinderling, *Langmuir* **2006**, 22, 3450.

- 1 224 M. J. Dalby, D. McCloy, M. Robertson, H. Agheli, D. Sutherland, S. Affrossman, R. O. Oreffo,
2 *Biomaterials* **2006**, *27*, 2980.
3
- 4 225 R. K. Silverwood, P. G. Fairhurst, T. Sjöström, F. Welsh, Y. Sun, G. Li, B. Yu, P. S. Young, B. Su,
5 R. M. Meek, M. J. Dalby, P. M. Tsimbouri, *Adv. Healthc. Mater.* **2016**, *5*, 947.
6
- 7 226 T. Sjostrom, L. E. McNamara, L. Yang, M. J. Dalby, B. Su, *ACS Appl. Mater. Interfaces* **2012**, *4*,
8 6354.
9
- 10 227 L. E. McNamara, T. Sjöström, K. E. Burgess, J. J. Kim, E. Liu, S. Gordonov, P. V. Moghe, R. M.
11 Meek, R. O. Oreffo, B. Su, M. J. Dalby, *Biomaterials* **2011**, *32*, 7403.
12
- 13 228 T. Sjostrom, N. Fox, B. Su, *Nanotechnol.* **2009**, *20*, 135305.
14
- 15 229 N. Gadegaard, M. J. Dalby, M. O. Riehle, A. S. G. Curtis, S. Affrossman, *Adv. Mater.* **2004**, *16*, 1857.
16
- 17 230 C. C. Berry, M. J. Dalby, R. O. Oreffo, D. McCloy, S. Affrosman, *J. Biomed. Mater. Res. A* **2006**,
18 79, 431.
19
- 20 231 H. M. Birch, *Nature* **2007**, *446*, 937.
21
- 22 232 A. Mata, E. J. Kim, C. A. Boehm, A. J. Fleischman, G. F. Muschler, S. Roy, *Biomaterials* **2009**, *30*,
23 4610.
24
- 25 233 M. J. Dalby, M. O. Riehle, H. Johnstone, S. Affrossman, A. S. Curtis, *Cell Biol. Int.* **2004**, *28*, 229.
26
- 27 234 L. E. McNamara, T. Sjöström, K. Seunarine, R. D. Meek, B. Su, M. J. Dalby, *J. Tissue Eng.* **2014**, *5*,
28 2041731414536177.
29
- 30 235 A. I. Teixeira, G. A. Abrams, P. J. Bertics, C. J. Murphy, P. F. Nealey, *J. Cell Sci.* **2003**, *116*, 1881.
31
- 32 236 R. K. Das, O. F. Zouani, C. Labrugere, R. Oda, M. C. Durrieu, *ACS Nano* **2013**, *7*, 3351.
33
- 34 237 E. A. Cavalcanti-Adam, T. Volberg, A. Micoulet, H. Kessler, B. Geiger, J. P. Spatz, *Biophys. J.* **2007**,
35 92, 2964.
36
- 37 238 J. Yang, L. E. McNamara, N. Gadegaard, E. V. Alakpa, K. V., Burgess, R. M. Meek, M. J. Dalby,
38 *ACS Nano* **2014**, *8*, 9941.
39
- 40 239 J. Malmstrom, J. Lovmand, S. Kristensen, M. Sundh, M. Duch, D. S. Sutherland, *Nano Lett.* **2011**,
41 11, 2264.
42
- 43 240 M. J. Biggs, R. G. Richards, N. Gadegaard, C. D. Wilkinson, R. O. Oreffo, M. J. Dalby, *Biomaterials*
44 **2009**, *30*, 5094.
45
- 46 241 C. S. Buensuceso, D. Woodside, J. L. Huff, G. E. Plopper, T. E. O'Toole, *J. Cell Sci.* **2001**, *114*,
47 1691.
48
- 49 242 M. J. Dalby, A. Hart, S. J. Yarwood, *Biomaterials* **2008**, *29*, 282-289.
50
- 51 243 N. Q. Balaban, U. S. Schwarz, D. Riveline, P. Goichberg, G. Tzur, I. Sabanay, D. Mahalu, S. Safran,
52 A. Bershadsky, L. Addadi, B. Geiger, *Nat. Cell Biol.* **2001**, *3*, 466.
53
- 54 244 T. Shemesh, B. Geiger, A. D. Bershadsky, M. M. Kozlov, *Proc. Natl. Acad. Sci. U. S. A.* **2005**, *102*,
55 12383.
56
- 57 245 A. J. Engler, S. Sen, H. L. Sweeney, D. E. Discher, *Cell* **2006**, *126*, 677.
58
- 59 246 R. McBeath, D. M. Pirone, C. M. Nelson, K. Bhadriraju, C. S. Chen, *Dev. Cell* **2004**, *6*, 483.
60
- 61 247 K. A. Kilian, B. Bugarija, B. T. Lahn, M. Mrksich, *Proc. Natl. Acad. Sci. U. S. A.* **2010**, *107*, 4872.
62
- 63 248 N. A. Patankar, *Langmuir* **2004**, *20*, 8209–8213.
64
- 65 249 M. Yamamoto, N. Nishikawa, H. Mayama, Y. Nonomura, S. Yokojima, S. Nakamura, K. Uchida,
Langmuir **2015**, *31*, 7355.
66
- 67 250 J. Ma, Y. Sun, K. Gleichauf, J. Lou, Q. Li, *Langmuir* **2011**, *27*, 10035.

- 1 251 J. K. Oh, X. Lu, Y. Min, L. Cisneros-Zevallos, M. Akbulut, *ACS Appl. Mater. Interfaces* **2015**, 7,
2 19274.
3
4 252 F. Hizal, N. Rungraeng, J. Lee, S. Jun, H. J. Busscher, H. C. Van der Mei, C. H. Choi, *ACS Appl.*
5 *Mater. Interfaces* **2017**, 9, 12118.
6
7 253 W. Choi, E. P. Chan, J. H. Park, W. G. Ahn, H. W. Jung, S. Hong, J. S. Lee, J. Y. Han, S. Park, D.
8 H. Ko, J. H. Lee, *ACS Appl. Mater. Interfaces* **2016**, 8, 31433.
9
10 254 E. Beltrán-Partida, B. Valdez-Salas, M. Curiel-Álvarez, S. Castillo-Urbe, A. Escamilla, N. Nedev,
11 *Mater. Sci. Eng.* **2017**, 76, 59.
12
13 255 C. Lüdecke, M. Roth, W. Yu, U. Horn, J. Bossert, K. D. Jandt, *Colloids Surf. B: Biointerfaces* **2016**,
14 145, 617.
15
16 256 J. Pang, T. Sjöström, D. Dynmock, B. Su, *Bioinspired, Biomimetic and Nanobiomaterials* **2013**, 2,
17 117.
18
19 257 S. Kim, Y. Zhou, J. D. Cirillo, A. A. Polycarpou, H. Liang, *J. Appl. Phys.* **2015**, 117, 155302.
20
21 258 E. Dayyoub, E. Belz, N. Dassinger, M. Keusgen, U. Bakowsky, *Phys. Status Solidi A* **2011**, 208,
22 1279.
23
24 259 C. Serrano, L. García-Fernández, J. P. Fernández-Blázquez, M. Barbeck, S. Ghanaati, R. Unger, J.
25 Kirkpatrick, E. Arzt, L. Funk and P. Turón, *Biomaterials* **2015**, 52, 291.
26
27 260 S. Liu, L. Wei, L. Hao, N. Fang, M. W. Chang, R. Xu, Y. Yang, Y. Chen, *ACS Nano* **2009**, 3, 3891.
28
29 261 E. P. Ivanova, J. Hasan, H. K. Webb, V. K. Truong, G. S. Watson, J. A. Watson, V. A. Baulin, S.
30 Pogodin, J. Y. Wang, M. J. Tobin, C. Løbbe, R. J. Crawford, *Small* **2012**, 8, 2489.
31
32 262 S. Pogodin, J. Hasan, V. A. Baulin, H. K. Webb, V. K. Truong, T. H. Phong Nguyen, V. Boshkovikj,
33 C. J. Fluke, G. S. Watson, J. A. Watson, R. J. Crawford, E. P. Ivanova, *Biophys. J.* **2013**, 104, 835.
34
35 263 S. M. Kelleher, O. Habimana, J. Lawler, B. O'Reilly, S. Daniels, E. Casey, A. Cowley, *ACS Appl.*
36 *Mater. Interfaces* **2015**, 8, 14966.
37
38 264 A. Elbourne, R. J. Crawford, E. P. Ivanova, *J. Colloid Interface Sci.* **2017**, 508, 603.
39
40 265 A. Tripathy, P. Sen, B. Su, W. H. Briscoe, *Adv. Colloid Interface Sci.* **2017**, 248, 85.
41
42 266 D. E. Mainwaring, S. H. Nguyen, H. Webb, T. Jakubov, M. Tobin, R. N. Lamb, A. H. F. Wu, R.
43 Marchan, R. J. Crawford, E. P. Ivanova, *Nanoscale* **2016**, 8, 6527.
44
45 267 V. K. Truong, N. M. Geeganagamage, V. A. Baulin, J. Vongsvivut, M. J. Tobin, P. Luque, R. J.
46 Crawford, E. P. Ivanova, *Appl. Microbiol. Biotechnol.* **2017**, 101, 4683.
47
48 268 F. Viela, I. Navarro-Baena, J. J. Hernández, M. R. Osorio, I. Rodríguez, *Bioinsp. Biomim.* **2018**, 13,
49 026011.
50
51 269 X. Li, G. S. Cheung, G. S. Watson, J. A. Watson, S. Lin, L. Schwarzkopf, D. W. Green, *Nanoscale*
52 **2016**, 8, 18860.
53
54 270 M. J. Hayes, T. P. Levine, R. H. Wilson, *J. Insect. Sci.* **2016**, 16, 1.
55
56 271 E. P. Ivanova, J. Hasan, H. K. Webb, G. Gervinskas, S. Juodkazis, V. K. Truong, A. H. F. Wu, R. N.
57 Lamb, V. A. Baulin, G. S. Watson, J. A. Watson, D. E. Mainwaring, R. J. Crawford, *Nat. Commun.*
58 **2013**, 4, 2838.
59
60 272 H. Hu, V. S. Siu, S. M. Gifford, S. Kim, M. Lu, P. Meyer, G. A. Stolovitzky, *Appl. Phys. Lett.* **2017**,
61 111, 253701.
62
63 273 D. P. Linklater, H. K. D. Nguyen, C. M. Bhadra, S. Juodkazis, E. P. Ivanova, *Nanotechnology* **2017**,
64 28, 245301.
65
66 274 A. Susarrey-Arce, I. Sorzabal-Bellido, A. Oknianska, F. McBride, A. Beckett, J. Gardeniers, R. Raval,
67 R. Tiggelaar, Y. D. Fernandez, *J. Mater. Chem. B* **2016**, 4, 3104.

- 1 275 L. E. Fisher, Y. Yang, M. F. Yuen, W. Zhang, A. H. Nobbs, B. Su, *Biointerphases* **2016**, *11*, 011014.
2
3 276 P. W. May, M. Clegg, T. A. Silva, H. Zanin, O. Fatibello-Filho, V. Celorrio, D. J. Fermin, C. C.
4 Welch, G. Hazell, L. Fisher, A. Nobbs, B. Su. *J. Mater. Chem. B* **2016**, *4*, 5737.
5 277 G. Hazell, P. W. May, P. Taylor, A. H. Nobbs, C. C. Welch, B. Su, *Biomater. Sci.* **2018**, *6*, 1424.
6 278 T. Diu, N. Faruqui, T. Sjöström, B. Lamarre, H. F. Jenkinson, B. Su, M. G. Ryadnov, *Sci. Rep.* **2014**,
7 *4*, 7122.
8
9 279 C. M. Bhadra, V. Khanh Truong, V. T. H. Pham, M. Al Kobaisi, G. Seniutinas, J. Y. Wang, S.
10 Juodkazis, R. J. Crawford, E. P. Ivanova, *Sci. Rep.* **2015**, *5*, 16817.
11 280 Y. Cao, B. Su, S. Chinnaraj, S. Jana, L. Bowen, S. Charlton, P. Duan, N. S. Jakubovics, J. Chen, *Sci.*
12 *Rep.* **2018**, *8*, 1071.
13 281 A. Jaggessar, A. Mathew, H. Wang, T. Tesfamichael, C. Yan, P. K. D. V Yarlagadda, *J. Mech. Behav.*
14 *Biomed. Mater.* **2018**, *80*, 311.
15 282 C. Sengstock, M. Lopian, Y. Motemani, A. Borgmann, C. Khare, P. J. S. Buenconsejo, T. A.
16 Schildhauer, A. Ludwig, M. Köller, *Nanotechnology* **2014**, *25*, 195101.
17 283 J. Hasan, S. Jain, K. Chatterjee, *Sci Rep* **2017**, *7*, 41118.
18 284 T. Sjöström, A. H Nobbs, B. Su, *Mater. Lett.* **2016**, *167*, 22.
19 285 M. N. Dickson, E. I. Liang, L. A. Rodriguez, N. Vollereaux, A. F. Yee, *Biointerphases* **2015**, *10*,
20 021010.
21 286 K. Minoura, M. Yamada, T. Mizoguchi, T. Kaneko, K. Nishiyama, M. Ozminskyj, T. Koshizuka, I.
22 Wada, T. Suzutani, *PLoS ONE* **2017**, *12*, e0185366.
23 287 F. Viela, I. Navarro-Baena, J. J. Hernández, M. R. Osorio, I. Rodrigues, *Bioinspir. Biomim.* **2018**, *13*,
24 026011.
25 288 G. Hazell, L. E. Fisher, W. A. Murray, A. H. Nobbs, B. Su, *J. Colloid Interface Sci.* **2018**, *528*, 389.
26 289 Y. Jang, W. T. Choi, C. T. Johnson, A. J. García, P. M. Singh, V. Breedveld, D. W. Hess, J. A.
27 Champion, *ACS Biomater. Sci. Eng.* **2018**, *4*, 90.
28 290 J. Hasan, S. Jain, R. Padmarajan, S. Purighalla, V. K. Sambandamurthy, K. Chatterjee, *Mater. Des.*
29 **2018**, *140*, 332.
30 291 P. A. Nistor, P. W. May, *J. R. Soc. Interface* **2017**, *14*, 20170382.
31 292 K. Kapat, P. P. Maity, A. P. Rameshbabu, P. K. Srivas, P. Majumdar, S. Dhara, *J. Mater. Chem. B* **2018**,
32 *6*, 2877.
33 293 V. Goriainov, G. Hulsart-Billstrom, T. Sjostrom, D. G. Dunlop, B. Su, R. O. C. Oreffo, *Front. Bioeng.*
34 *Biotechnol.* **2018**, *6*, 44.
35 294 M. Fernandez-Fairen, A. Torres, A. Menzie, D. Hernandez-Vaquero, J. M. Fernandez-Carreira, A.
36 Murcia-Mazon, E. Guerado, L. Merzthal, *Open Orthop. J.* **2013**, *7*, 227.
37 295 X. Wang, T. Lu, J. Wen, L. Xu, D. Zeng, Q. Wu, L. Cao, S. Lin, X. Liu, X. Jiang, *Biomaterials* **2016**,
38 *83*, 207.
39 296 V. T. Pham, V. K. Truong, A. Orłowska, S. Ghanaati, M. Barbeck, P. Booms, A. J. Fulcher, C. M.
40 Bhadra, R. Buividas, V. Baulin, C. J. Kirkpatrick, P. Doran, D. E. Mainwaring, S. Juodkazis, R. J.
41 Crawford, E. P. Ivanova, *ACS Appl. Mater. Interfaces* **2016**, *8*, 22025.
42 297 P. M. Tsimbouri, L. Fisher, N. Holloway, T. Sjostrom, A. H. Nobbs, R. M. Meek, B. Su B, M. J.
43 Dalby, *Sci. Rep.* **2016**, *6*, 36857.
44 298 R. Fraioli, P. M. Tsimbouri, L. E. Fisher, A. H. Nobbs, B. Su, S. Neubauer, F. Rechenmacher, H.
45 Kessler, M. P. Ginebra, M. J. Dalby, J. M. Manero, C. Mas-Moruno, *Sci. Rep.* **2017**, *7*, 16363.
46
47
48
49
50
51
52
53
54
55
56
57
58
59
60
61
62
63
64
65

1 ²⁹⁹ J. N. Roberts, J. K. Sahoo, L. E. McNamara, K. V. Burgess, J. Yang, E. V. Alakpa, H. J. Anderson,
2 J. Hay, L.-A. Turner, S. J. Yarwood, M. Zelzer, R. O. C. Oreffo, R. V. Ulijn, M. J. Dalby, *ACS Nano*
3 **2016**, *10*, 6667.

4
5 ³⁰⁰ M.-H. Xiong, Y.-J. Li, Y. Bao, X.-Z. Yang, B. Hu, J. Wang, *Adv. Mater.* **2012**, *24*, 6175.

6
7 ³⁰¹ G. D. Wright, *Nat. Prod. Rep.* **2017**, *34*, 694.

8
9 ³⁰² O. Genilloud, *Nat. Prod. Rep.* **2017**, *34*, 1203.

10
11 ³⁰³ M. K. Kim, A. Zhao, A. Wang, Z. Z. Brown, T. W. Muir, H. A. Stone, B. L. Bassler, *Nature Microbiol.*
12 **2017**, *2*, 17080.



Click here to access/download
Production Data
Bios all authors.docx





Click here to access/download
Production Data
TOC.docx